ISTANBUL TECHNICAL UNIVERSITY ★ GRADUATE SCHOOL

COMPUTATION OF THERMAL CONDUCTIVITY IN NANOFLUIDS

M.Sc. THESIS

Ceren Ece YÜCE

Department of Physics Engineering

Physics Engineering Programme

JANUARY 2023

ISTANBUL TECHNICAL UNIVERSITY ★ GRADUATE SCHOOL

COMPUTATION OF THERMAL CONDUCTIVITY IN NANOFLUIDS

M.Sc. THESIS

Ceren Ece YÜCE
(509191127)

Department of Physics Engineering

Physics Engineering Programme

Thesis Advisor: Assoc. Prof. Cem SERVANTIE

JANUARY 2023

İSTANBUL TEKNİK ÜNİVERSİTESİ ★ LİSANSÜSTÜ EĞİTİM ENSTİTÜSÜ

NANOAKIŞKANLARDA ISI İLETKENLİĞİ HESAPLAMALARI

YÜKSEK LİSANS TEZİ

Ceren Ece YÜCE
(509191127)

Fizik Mühendisliği Anabilim Dalı

Fizik Mühendisliği Programı

Tez Danışmanı: Doç. Dr. Cem SERVANTIE

OCAK 2023

Ceren Ece YÜCE, a M.Sc. student of ITU Graduate School student ID 509191127, successfully defended the thesis entitled " COMPUTATION OF THERMAL CONDUCTIVITY IN NANOFLUIDS", which she prepared after fulfilling the requirements specified in the associated legislations, before the jury whose signatures are below.

Thesis Advisor :	**Assoc. Prof. Cem SERVANTIE** Istanbul Technical University	.....
Jury Members :	**Prof. Dr. Sevim İşçi TURUTOĞLU** Istanbul Technical University	.....
	Asst. Prof. Ayşe ULUBAY Istanbul University	.....

Date of Submission : 26 December 2022
Date of Defense : 17 January 2023

To my family,

FOREWORD

This master thesis study was carried out under the consultancy of Assoc. Prof. Cem Servantie. I want to express my gratitude to my adviser Assoc. Prof. Cem Servantie who supported and assisted me during my studies. I can express the extent of my gratitude to Prof. Assoc. Prof. Cem Servantie for great patience during my work. Without his assistance and knowledge, I would not have been successful in this work.

I offer my gratitudes to my family who are always by my side and give their endless love.

January 2023 Ceren Ece YÜCE

TABLE OF CONTENTS

ABBREVIATIONS

MD	**:** Molecular Dynamics
EMD	**:** Equilibrium Molecular Dynamics
NEMD	**:** non-Equilibrium Molecular Dynamics
rNEMD	**:** Reverse non-Equilibrium Molecular Dynamics
HCAF	**:** Heat Current Auto-Correlation Function
Q-SC	**:** quantum corrected Sutton-Chen
FENE	**:** Finitely Extensible Non-Linear Elastic
LJ	**:** Lennard-Jones
DT	**:** Dual Thermostat
MP	**:** Müller-Plathe
EAM	**:** Embedded Atom Modelling

SYMBOLS

k_b	: Boltzmannn constant
a	: Lattice constant
t	: Time
E	: Energy
P	: Momentum
m	: Mass
v	: Velocity
V	: Volume
ρ	: Density
σ	: Characteristic length scale
ε	: Strength of interaction
r_c	: Cutoff distance
Pt	: Platinum
K	: Kelvin
λ	: Thermal conductivity coefficient

LIST OF TABLES

Page

LIST OF FIGURES

Page

COMPUTATION OF THERMAL CONDUCTIVITY IN NANOFLUIDS

SUMMARY

Molecular dynamics simulation is a popular computational technique that is widely used to simulate and investigate thermophysical properties of nanofluids. Molecular dynamics is frequently used in chemical physics, materials science, and molecular-scale modeling because it offers an atomistic level understanding of the equation of transport coefficient. The most common method is with the use of the Green-Kubo relation, with equilibrium molecular dynamics. The other well known method is by non-equilibrium simulations by either imposing a gradient of temperature by modifying the boundaries or by the use of the so-called thermal force.

Experiments suggest nanofluids have enhanced heat transfer coefficient compared to the base fluid. That make nanofluids beneficial in a wide range of industrial and home heat transfer applications, including as engine cooling and vehicle thermal management, fuel cells, microelectronics, heat exchangers in boilers and refrigerators, and solar water heaters.

In this thesis we evalute the thermal conductivity of a nanofluid with different molecular dynamics methods. The simulations run under the NVE conditions, for which the total atom number, total volume, and total energy are constant. Using the cell list approach, we create neighbor lists to increase computing efficiency. The Velocity Verlet technique is then used to integrate the equations of motion with a time step of 0.001. Since they are both conserved quantities, the total energy E and the total momentum **P** are computed to test the code. Throughout all of the simulations, the temperature and density of box are taken to be 0.722 and 0.8442 in dimensionless units, respectively.

For the fluid-fluid, fluid-nanoparticle, and nanoparticle-nanoparticle interactions the Lennard-Jones potential is used while for the interatomic interactions in the nanoparticles we used the quantum corrected Sutton-Chen (Q-SC) many body potential. The volume fraction of the nanoparticles is varied from 0.3% to 9%. We used two different reverse non-equilibrium molecular dynamics (rNEMD) methods to evaluate the thermal conductivity of the nanofluid. Namely, the velocity exchange method and dual thermostat method. In the velocity exchange method the total energy and linear momentum are conserved while for the dual thermostat method the total energy and linear momentum are not conserved. The difference between rNEMD methods and the traditional non-equilibrium (NEMD) methods is that a heat flux is imposed on the system and then the temperature gradient is measured. This has two main advantages, first of all the heat flux is not well defined for systems with many-body interactions, secondly when one imposes a temperature gradient by

modifying the periodic boundaries, this results in surface effects. However, for the rNEMD simulations the heat flux is imposed by unphysical means, and one must be careful in the interpretation of the results.

The velocity exchange method and dual thermostat method results show that for a volume fraction of 0.3% of nanoparticles the thermal conductivity slightly increased while for larger volume fractions the thermal conductivity decreases.

NANOAKIŞKANLARDA ISI İLETKENLİĞİ HESAPLAMALARI

ÖZET

Sıvılar, ısıtma ve soğutma sistemlerinde yaygın olarak kullanılmaktadır. Sıvıların bu alanlardada verimliliğini artırma yaklaşımları günümüzde araştırmacıların temel amacıdır.

Nanoakışkan, yeni termik akışkan, sıvının içinde nano boyutta parçacık olması durumuna denir. Mikro boyutlu parçacıklar içeren sıvılardan ziyade nano boyutlu parçacıklar içeren sıvılar daha kararlıdır. Çünkü mikro boyutlu parçacıklar çökelme ve tortulaşma gibi sorunlara neden olabiliyor. Nanoakışkanlar, çeşitli ısı transfer uygulamalarında ısı transfer sıvılarının geleceği olarak düşünülebilir. Nanoakışkan üretiminde genellikle kullanılan nanoparçacıklar metaller, oksitler, karbon nanotüpler vb iken genellikle kullanılan sıvılar argon, su, etilen glikol, yağ vb dir. Yüksek termal iletkenliğe sahip asılı nanoparçacıkların varlığı nedeniyle ve nano boyutta yaptıkları titreşim hareketiyle ve çevresindeki sıvı moleküllerinde oluşturduğu hareket sayesinde geleneksel akışkanlardan daha iyi termal performans göstermeleri beklenir. Spesifik termofiziksel özellikler elde etmek için nanoakışkanlar hakkında yapılan son çalışmalar, termal iletkenliği etkileyen çeşitli faktörlerin daha iyi anlaşılmasına duyulan ihtiyacın artmasına neden oldu. Termal iletkenlik, nanoparçacıkların boyutu, nanoparçacığın maddesi, nanoparçacıkların şeklinin tipi, nanoparçacıkların hacim oranı ve sıvının özellikleri gibi çeşitli parametrelere bağlıdır. Bu parametreler termal iletkenliği artırabilir veya azaltabilir. Nanoakışkanların kullanım alanları yüksek ısı iletkenlikleri ve bu durumun arkasındaki fiziğin daha iyi anlaşılmasından dolayı yüksek ısı akılı yüzeylerden olan ısı transferi uygulamalarında olmak üzere, otomotiv sanayii, elektronik cihazların ekranları, bilgisayarlar ve buzdolapları sıralanabilir.

Nanoakışkanlar literatürde deneysel ve empirik olarak çalışılmasından ziyade nümerik şekilde de çalışılmıştır. Nanoakışkanın üretim ve finansal zorluğu literatürdeki deneyler arasındaki uyuşmazlık ve kullanılan deneysel tekniklerin çeşitliliği gibi sebepler nedeniyle nümerik çalışmalar daha da yaygınlaşmıştır.

Moleküler dinamik (MD) simülasyon, istatistiksel mekaniğe dayalı bir bilgisayar simülasyon yöntemidir. Hem katı hem de sıvı atomlar arasındaki atomik seviye etkileşimlerini gözlemleyerek katıların ve sıvıların statik ve dinamik özellikleri hakkında bilgi almak için moleküler dinamik simülasyonu kullanılabilir. Moleküler dinamik simülasyonu ile her seferinde moleküler konum ve momentum hakkında bilgi sahibi olabiliriz, ayrıca nanoparçacıkların şekli kontrol edilebilir. Moleküler dinamik simulasyonun çalışma prensibi, verilen başlangıç konumları ve başlangıç hızları ile, diğer tüm atomlar tarafından her bir atom üzerindeki kuvveti hesaplayabiliriz. Sonra Newton'un ikinci hareket yasasını kullanarak atomların konumlarını ve hızlarını

güncelleyebiliriz. Zaman artırılır ve istenen zamana ulaşılana kadar kuvvetler hesaplanarak döngü tekrarlanır. Moleküler dinamik simulasyon, nanoakışkanların termal iletkenliğini değerlendirmek için kullanışlı bir araçtır. Tıpkı deneysel çalışsmalardaki gibi, önce N parçacık içeren model sistem seçilir ve örnek hazırlanır. Daha sonrasında termal dengeye ulaşan sistemin ölçümleri alınır.

Bu çalışmada denge durumundaki nanoakışkanın termal iletlenlik katsayısı hesaplanmaktadır. Termal iletkenlik Fourier Yasası ile ifade edilir. Termal iletkenliği ölçmek için en yaygın kullanılan yöntem, denge moleküler dinamik simülasyon yöntemidir. Denge moleküler dinamik simulasyon yönteminde Green-Kubo ilişkisi kullanılır. Green-Kubo yöntemi mikroskopik ısı akısının zaman oto-korelasyon fonksiyonun integraline dayanır. Diğer en yaygın kullanılan yöntemlerden biri ise, ya sınırları değiştirerek bir sisteme sıcaklık gradyanı empoze ederek ya da termal kuvvet denen şeyi kullanarak denge dışı moleküler dinamik simülasyonlardır.

Bu tez çalışmasında, metalik nanoparçacıkların hacimsel katkısının termal iletlenliğe etkisi baz sıvının termal iletkenliği ile karşılaştırılarak değerlendimek için moleküler dinamik simülasyon yöntemleri kullanıldı. Baz akışkan olarak Lennard Jones akışkanı modellenmiştir. Farklı hacimsel katkılardaki 4 nanoakışkan modeli için toplam 4 farklı set hazırlanmış ve denge konumuna getirebilmek için her bir set ilk olarak 10^6 adım çalıştırılmıştır. Bu setler tek nanoparçacık için 0.3%, 10 nanoparçacık icin 3%, 20 nanoparçacık için 6%, 30 nanoparçacık için 9% hacim katkısına sahiptir. Sıvı-sıvı, sıvı-nanoparçacık ve nanoparçacık-nanoparçacık etkileşimleri için Lennard-Jones potansiyeli kullanılırken, metalik nanoparçacıklardaki atomlar arası etkileşimler için ise kuantum düzeltmeli Sutton-Chen (Q-SC) potansiyeli kullanıldı. Metaller ve alaşımlar için, Sutton-Chen potansiyeli en yaygın kullanılan potansiyellerden biridir. Simulasyon boyunca toplam atom sayısı, sistemin hacmi ve sistemin toplam enerjisinin korunduğu mikrokanonik kümede çalışılmıştır. Atomların konumlarını belirleyebilmek için Velocity Verlet algoritması kullanılmıştır.

Metalik nanoparçacıklara sahip farklı hacim katkılarındaki nanoakışkanların ısıl iletkenliği, üç farklı yöntem kullanılarak hesaplanmıştır. Bu yöntemler denge moleküler dinamik simülasyon, hız değişim yöntemi ve çift termostat yöntemi olmak üzere farklı hacim katkılarındaki nanoakışkanların ısıl iletkenliği hesaplanmıştır. Aynı zamanda baz sıvının ısıl iletkenliği de hesaplanmıştır ve baz sıvının termal iletkenliği nanoakışkanların termal iletkenliği ile karşılaştırılmıştır.

Çift termostat yönteminde iki farklı dinlenme süresi kullanılarak farklı hacim katkılarındaki nanoakışkanların termal iletkenliği hesaplanmıştır. Bu yöntemde enerji korunmamıştır. İki farklı dinlenme süresi için de sonuçlar % 0.3 hacim katkısındaki nanoakışkan için termal iletkenliğin arttığını göstermiştir. Ama daha büyük hacim kakısındaki nanoakışkanların ısıl iletkenliğinde artış gözükmemiş hatta düşüş gözlemlenmiştir.

Hız değişim yönteminde üç farklı dinlenme zamanı kullanılmıştır. Bu yöntemde enerji ve momentum korunmuştur. İki dinlenme zamanı için %0.3 hacim katkısındaki nanoakışkanın termal iletkenliğinde yükselme gözlenirken diğer dinlenme zamanı için gözlemlenememiştir.

Denge moleküler simülasyon yöntemiyle baz sıvı, 0.3% hacim katkısındaki nanoakışkanın ve 9% hacim katkısındaki nanoakışkanın termal iletkenliği hesaplanmıştır. Bu yöntemde bulduğumuz sonuçlar ise çift termostat yöntemi ve hız değişim yönteminde bulduğumuz sonuçlar ile çelişmektedir. Denge moleküler simülasyon yönteminde, %0.3 ve %9 hacim katkılarındaki nanoakışkanların termal iletkenliğinde artış gözlemlenmiştir.

1. INTRODUCTION

1.1 Molecular Dynamics Simulation

A "Simulation," as defined by Oxford Dictionary (2017), is the "imitation of a situation or process," or "the action of pretending; deception," or "the production of a computer model of something, especially for the purpose of study [1]. Molecular Dynamics (MD) simulation method is a computer simulation method based on statistical mechanics and it was first used at the end of the 1950s by Alder and Wainwright [3]. They studied with an IBM 704 computer to simulate perfectly elastic collisions that occurred between hard spheres.

Molecular Dynamics analysis the physical movements of atoms and molecules. We can use Molecular Dynamic simulation to get information about static and dynamic properties of solids and liquids by observing the atomic level interactions between both atoms. We can be informed about molecular position and momentum at each time with the Molecular Dynamics (MD) simulation. Also, the shape of nanoparticles can be controlled.

Basically, the equations of motion follow from Newton's second law,

$$\mathbf{F}_i = m_i \frac{d^2\mathbf{r}_i}{dt^2}, (i = 1, 2, ..., N) \tag{1.1}$$

F refers the total force on the i^{th} atom, m is mass of an atom, and $\frac{d^2 r_i}{dt^2}$ is acceleration.

Figure 1.1 shows the working principle of MD simulation. With the given initial positions and initial velocities of atoms, we can compute the force on each atom due to all the other atoms. Then, by applying Newton's second law we can update positions and velocities of atoms. The time is incremented and the cycle repeats by computing the forces until the desired time is reached. Most common softwares for MD simulations are LAMMPS [4], AMBER [5], etc.

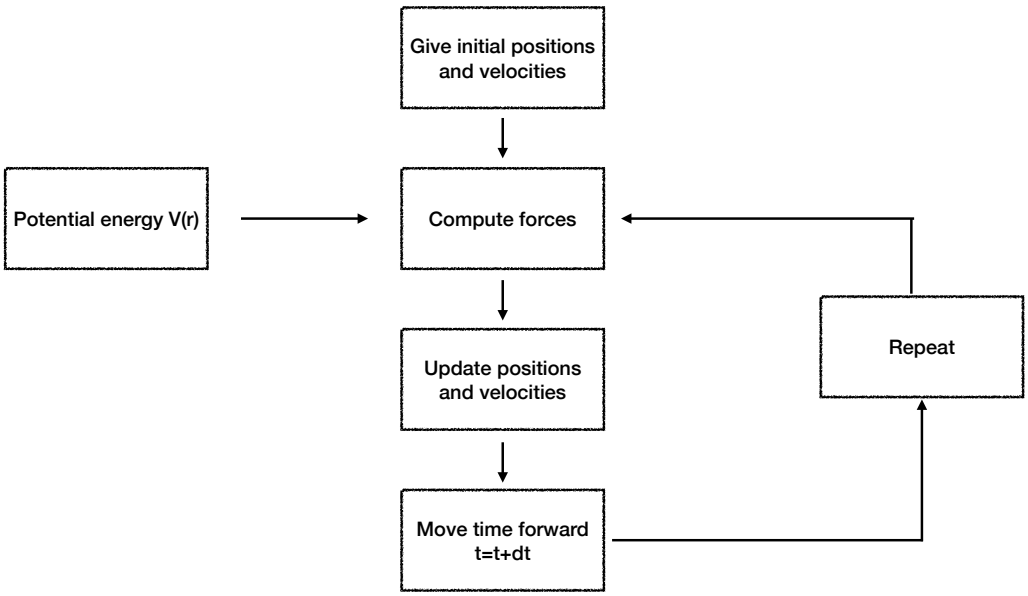

Figure 1.1 : Simple algorithm for Molecular Dynamics. The process is repeated until the desired time is reached.

Nejatolahi *et al.* [6] calculated the thermal conductivity of nanofluid with EMD and NEMD methods. They compared the results of traditional EMD and NEMD methods. They found that the EMD method is not in the acceptable range, however NEMD results are more reliable.

Recently, Müller-Plathe [7] proposed a novel method to evaluate thermal conductivity, namely the rNEMD method. Unlike the usual non-equilibrium molecular dynamics (NEMD) methods, here the heat flux is imposed instead of the gradient of temperature. Hence avoiding the problem of the evaluation of the heat flux for systems with many-body interactions. Moreover, with the so-called velocity exchange rNEMD method the total energy of the system is conserved. Later, Terao *et al.* [8] evaluated thermal conductivity of amorphous polymers with two different rNEMD, namely the dual thermostat (DT) and heat injection (HI) methods. Their results show that both methods are efficient for evaluating the thermal conductivity. Moreover, they observed that the thermal conductivity depends on the number of degrees of freedom in the model.

Wen *et al.* [9] investigated the thermal characteristics of platinum (Pt) nanoparticles with cube, octahedron, truncated octahedron, and sphere shapes by using the

Sutton-Chen potential during the heating process by molecular dynamics simulation. They showed that octahedron-truncated nanoparticle displays a better thermal stability than other polyhedral nanoparticles.

Recent molecular dynamics studies [10,11] showed thermal conductivity increases with the volume fraction of nanoparticles.

Sankar et al. [12] calculated thermal conductivity of nanofluid with Pt nanoparticle with various volume fraction. They used LJ potential for water-water, water-Pt interaction, and used Finitely Extensible Non-Linear Elastic (FENE) potential for the atoms inside metallic nanoparticles. They showed that with the increase at the volume fraction the thermal conductivity increased.

1.2 Nanofluids

Fluids are used as heat carriers in heat transfer equipment such as in cooling systems in buildings, and industrial process heating and cooling systems in petrochemical, textile, pulp and paper, chemical, food, and other processing plants [13]. Numerous experiments are done to investigate the heat transfer performance of traditional fluids. The idea of adding solids with spherical shape into fluids was first proposed by Maxwell [14]. However, due to the large size and high density of the particles, there is no good way to prevent the solid particles from settling out of suspension. After the first experimental evidence [15] with alumina nanoparticles in water, nanofluids has become increasingly interested. Mesuda *et al.* [15] observed that adding as little as 4.3% of silica, alumina, and other oxides to water enhanced the thermal conductivity of nanofluids by 30%. The three methods for studying nanofluids are experimental, empirical, and numerical. Scientists studied nanofluids with numerical models in order to address basic concerns because of the wide variety of experimental approaches and the significant inconsistencies between these investigations. Numerous materials have been used for nanoparticles with various base fluids, and the outcomes are remarkably variable for various combinations [16].

Nanofluids are a new class of heat transfer fluids that are binary mixtures that consist of nanometer-sized particles, i.e. metals, oxides, carbon nanotubes, which are suspended

in liquids such as argon, water, ethylene glycol and oil. Most of early studies were milli or micro-sized particles dispersions in the base fluid. However, micro sized particles led to sedimentation of the particles [14]. The term "nanofluid" was first proposed by Choi and Eastman in 1995 of the Argonne National Laboratory, U.S.A with the aim of increasing the thermal conductivity of heat transfer fluids [13]. First problem they faced in *R&D* program was the clogging problem with the micro sized particles, however nano sized particles will not have that problem. They showed that nanofluids have ability to increase heat transfer performance.

Recent studies about the nanofluids to get specific thermophysical properties have led to an increase in the need for a better understanding of the various factors that affect thermal conductivity [17]. Thermal conductivity depends on various parameters such as size of nanoparticle, type of nanoparticle shape of nanoparticles, and volume fraction of nanoparticle and properties of base fluid. These parameters can either increase or decrease thermal conductivity.

Most studies suggest that with the increase in volume fraction of nanoparticle, thermal conductivity increased. Eastman *et al.* [18] observed that thermal conductivity increased 40% with a volume fraction of 0.3% copper nanoparticles in the ethylene glycol. In fact, Patel *et al.* [19] showed that, even at the same surface to volume ratio, the thermal conduction enhancement differs for the particles that made of different materials.

Bahiraei [20] reviewed studies about particle migration in nanofluids and showed that nanofluids are promising in application of refrigeration techniques.

Moreover, temperature has an essential role in the enhancement of thermal conductivity of nanofluids. Increase in temperature leads to increase in the thermal conductivity. Mohebbi [21] evaluated thermal conductivity of 4.15% nanofluids at temperatures of $140.132K$ and $107K$, and results showed that with the increase in the temperature thermal conductivity of nanofluid decreased.

Murshed *et al.* [22] experimentally studied that nanofluids with spherical nanoparticles have a smaller increase in thermal conductivity than the nanofluids with the cylindirical nanoparticles. Then, they compared their experimental results with the several

theoretical models and found that experimental results are not consistent with the theoretical models.

Some researchers' studies showed that the thermal conductivities of nanofluids were strongly dependent on the size of the nanoparticles. Kim *et al.* [23] experimentally showed that size reduction increases the thermal conductivity. Thermal conductivities decreasing with increasing nanoparticle sizes, On the other hand, some researchers' results showed that the larger size particles gave the enhancement in thermal conductivity as compared to the lower nanoparticles.

In the present work, thermal conductivity of nanofluids with metallic nanoparticles is calculated at different volume fractions by applying equilibrium method and two different reverse non-equilibrium methods namely velocity exchange method and dual-thermostat method.

2. MODEL AND SIMULATION DETAILS

2.1 Model

The base fluid is modeled as a Lennard-Jones (LJ) fluid. The Lennard-Jones-type r^{ν} - r^{μ} pair potentials were first proposed in 1925 by Jones [24]. The 12-6 form was proposed by Lennard-Jones in 1931 after London had derived that the dispersion interaction between atoms decays as $\frac{1}{r^6}$ [25]. The Lennard Jones potential can be used in systems which are in the solid, liquid or gaseous states [26].

Even though the Lennard-Jones potential is commonly used for modelling liquid argon in most of the molecular dynamics simulation studies, it also has been chosen as a general interaction potential for studies not involving specific substances, we are interested in universal properties as in this work, therefore for the fluid-fluid, nanoparticle-fluid, also for the nanoparticle-nanoparticle interactions Lennard-Jones potential is used [27,28].

The 6-12 Lennard-Jones potential is written as,

$$\mathscr{V}_{LJ}(r) = \begin{cases} 4\varepsilon \left[\left(\frac{\sigma}{r}\right)^{12} - \left(\frac{\sigma}{r}\right)^{6} \right] & r < r_c \\ 0 & r > r_c \end{cases} \tag{2.1}$$

where ε refers to the well depth, it is a measure of the strength of the interaction between atoms, σ refers to the distance when the potential between two atoms is zero. The first term in equation 2.1 in the left represents the repulsive attraction while the second term represents the attractive attraction. The power 6 represents the van der Waals forces regarding London forces and dipole-dipole interactions in quantum mechanics while the power 12 is chosen only for mathematical convenience independently of any physical basis. Where the cut-off distance is taken as $r_c = 2.5\sigma$. For atoms further report, the Lennard Jones potential is negligible as depicted in Figure

2.1 [28]. Additionally, the Lennard-Jones parameters are fixed to unity, $\varepsilon = 1$ and $\sigma = 1$. The mass of the particles is also fixed to unity m=1.

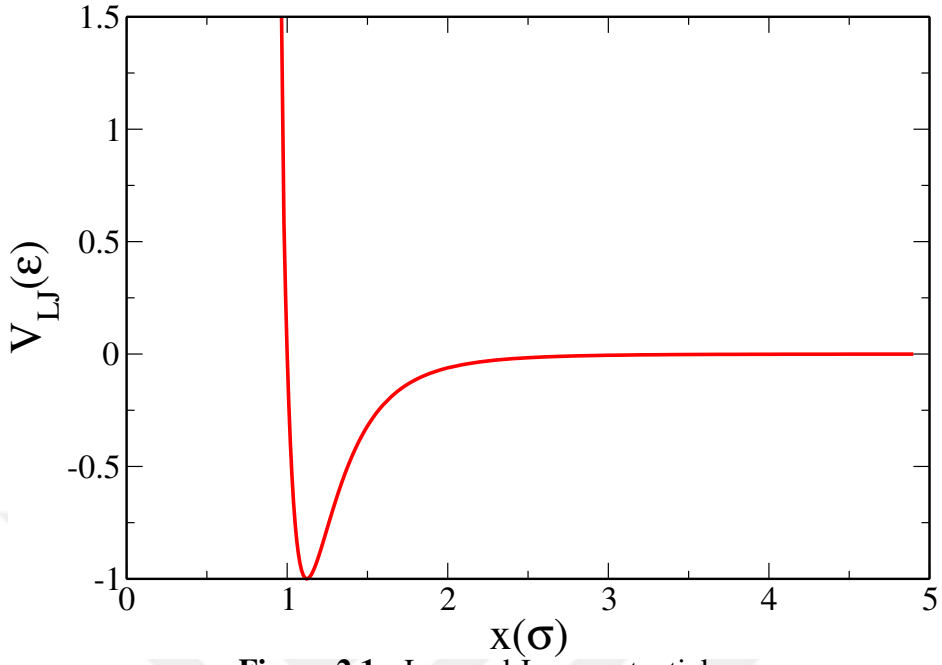

Figure 2.1 : Lennard Jones potential

The corresponding force is $\mathbf{F} = -\nabla \mathscr{V}_{LJ}$,

$$\mathbf{F}_{LJ}(r) = \begin{cases} \frac{24\varepsilon}{\sigma}\left[2\left(\frac{\sigma}{r}\right)^{13} - \left(\frac{\sigma}{r}\right)^{7}\right]\hat{\mathbf{r}} & r < r_c \\ 0 & r > r_c \end{cases} \tag{2.2}$$

For the metallic nanoparticles we used the quantum corrected Sutton-Chen (Q-SC) many body potential, which is a version of Embedded Atom Modelling (EAM), to describe interatomic interactions. The embedded-atom method is a semi-empirical, many-atom potential for computing the total energy of a metallic system [29]. Daw and Baskes [30,31] proposed the embedded-atom method.

$$E_{coh} = \sum_i G_i\left(\sum_{j\neq i}\rho_j^a(R_{ij})\right) + \frac{1}{2}\sum_i\sum_{j\neq i}U_{ij}(R_{ij}) \tag{2.3}$$

where the G is the embedding energy, ρ^a is the spherically averaged atomic electron density, and U is an electrostatic, two atom interaction.

The Sutton-Chen potential for one particle is [32],

$$U_i = \frac{1}{2}\sum_{j\neq i}^{N} V(r_{ij}) - c\sqrt{\rho_i} \tag{2.4}$$

where r_{ij} is the distance between i and j atoms. ρ_i is the local electron density and is given as,

$$\rho_i = \sum_{j \neq i}^{N} \phi(r_{ij}) = \sum_{j}^{N} \left(\frac{a}{r_{ij}} \right)^m \tag{2.5}$$

$V(r_{ij})$ is a pairwise repulsive potential

$$V(r_{ij}) = \left(\frac{a}{r_{ij}} \right)^n \tag{2.6}$$

The total potential is written as,

$$\mathscr{V}_{SC} = \sum_{i}^{N} U_i = \sum_{i}^{N} \varepsilon \left[\frac{1}{2} \sum_{j \neq i}^{N} V(r_{ij}) - c\sqrt{\rho_i} \right] \tag{2.7}$$

where the first term represents repulsion between atomic cores and the second term represents the bonding energy due to the electrons. c is a dimensionless parameter which scales the attractive terms. m and n are integer parameters. The parameters are set to $\varepsilon = 1$, $c = 71.336$, $a = 1.107$, $m = 11$, $n = 7$.

The total force can be written as,

$$\mathbf{F}_i = \sum_{j} \mathbf{F}_{ij} \tag{2.8}$$

$\mathbf{F}_{ij}$ is force between the i and j atoms.

$$\mathbf{F}_{ij} = -\varepsilon \sum_{i<j}^{N} \left[n \left(\frac{a}{r_{ij}} \right)^n - \frac{1}{2} cm \left(\frac{1}{\sqrt{\rho_i}} + \frac{1}{\sqrt{\rho_j}} \right) \left(\frac{a}{r_{ij}} \right)^m \right] \frac{\mathbf{r}_{ij}}{r_{ij}^2} \tag{2.9}$$

Equilibrated nanoparticle by using Sutton Chen potential is seen in Figure 2.2. It consist of 100 atoms with the radius of 2σ.

The volume fraction of nanoparticles in the dispersion is

$$\varphi = N \frac{V_N}{V} \tag{2.10}$$

where N and V_N are respectively the number and volume of nanoparticle, and where V the total volume.

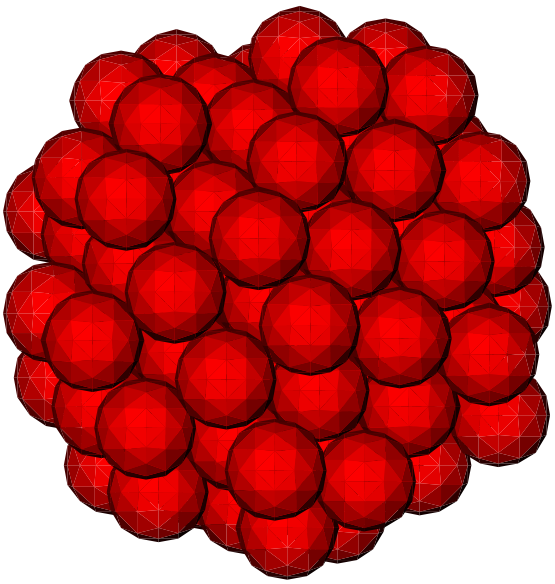

Figure 2.2 : Equilibrated metallic nanoparticle with a radius of 2σ.

Since the nanoparticles are spherical one can write $V_N = \frac{4}{3}\pi r_{eff}^3$ where r_{eff} is an effective radius which can be evaluated from the fluid particle nanopatcile radial distribution function g(r). According to Figure 2.3 first peak gives the the effective radius of nanoparticle and it is taken as 2.65σ. In order to have same fluid density, volume of the box is changed according to volume of the nanoparticles.

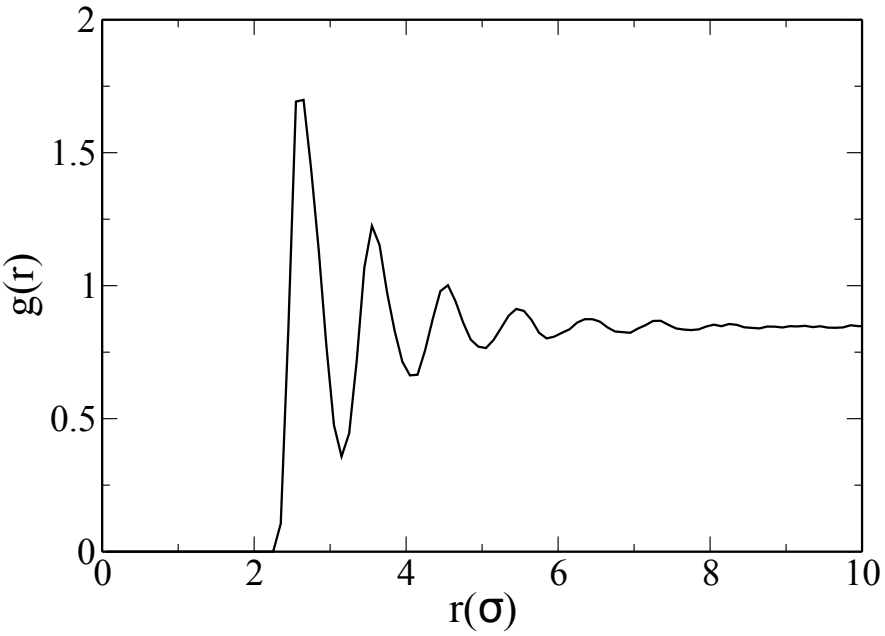

Figure 2.3 : Radial distribution function of a nanofluid with 0.3% volume fraction.

2.2 Simulation Details

2.2.1 Initial Configurations

The initial configuration of our bulk fluid system composed of 20000 atoms can be seen in Figure 2.4.

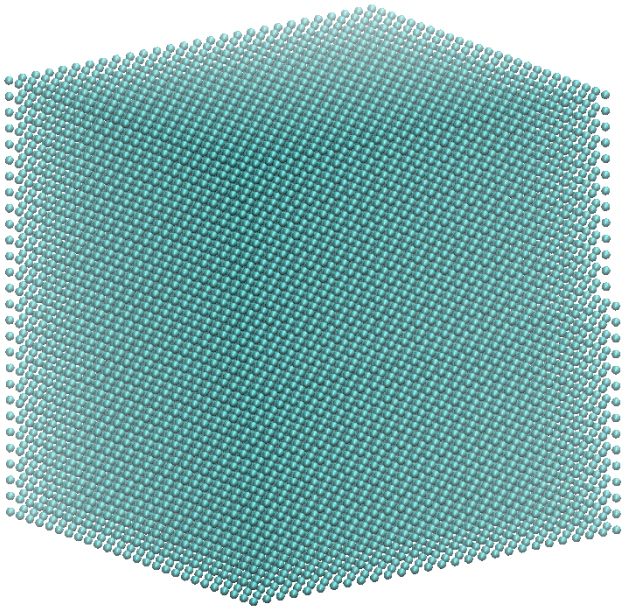

Figure 2.4 : Initial configuration of basefluid

Maxwell - Boltzmann distribution

$$\rho(v) = \left(\frac{m}{2\pi k_B T}\right)^{1/2} exp\left(-\beta\frac{1}{2}mv^2\right) \tag{2.11}$$

Prior to running the simulations, a velocity rescaling operation is carried out to modify the system temperature.

The metallic particles are arranged in a regular FCC lattice as spherical molecules that consist of 100 atoms and radius of nanoparticle is 2σ. 20000 fluid atoms are arranged in a simple cubic lattice. The size of box is 28.7σ in x, y and z directions. The initial velocities of atoms are set randomly with a Maxwell-Bolttzmann distribution. First, nanoparticles are constructed and equilibrated in a separate molecular dynamics simulation, then they are added to base fluid. Four different simulation boxes are constructed with volume fractions of 0.3%, 3%, 6%, 9% nanoparticles. Periodic

boundaries are applied in all directions. The velocity verlet integration algorithm is used with a time step of where $dt = 0.001\tau$ where $\tau = 2.161ps$. The temperature and density are taken as $k_bT = 0.722\varepsilon$ and $\rho = 0.8442\sigma^{-3}$ respectively. The dispersions are then equilibrated for 10^6 time steps during which velocity rescaling is imposed in order to have the desired temperature. An example of equlibrated simulation box is in Figure 2.5.

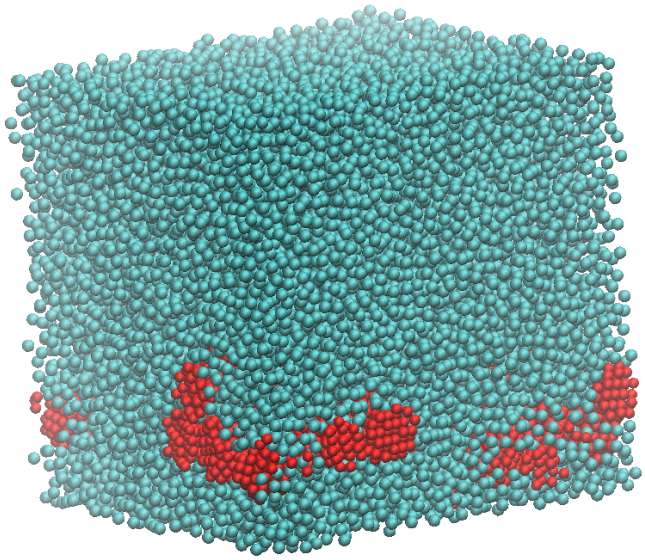

Figure 2.5 : Equilibrated nanofluid with a volume fraction of 9% nanoparticles.

2.2.2 Velocity Verlet Algorithm

The verlet integration is a numerical method used to integrate Newton's equations of motion. The verlet algorithm is derived from the Taylor expansions as follows,

$$r(t+\delta t) = r(t) + \frac{dr(t)}{dt}\delta t + \frac{1}{2}\frac{d^2r(t)}{dt^2}\delta t^2 + \frac{1}{3!}\frac{d^3r(t)}{dt^3}\delta t^3 + \mathscr{O}\left(\delta t^4\right) \tag{2.12}$$

$$r(t-\delta t) = r(t) - \frac{dr(t)}{dt}\delta t + \frac{1}{2}\frac{d^2r(t)}{dt^2}\delta t^2 - \frac{1}{3!}\frac{d^3r(t)}{dt^3}\delta t^3 + \mathscr{O}\left(\delta t^4\right) \tag{2.13}$$

Then, adding these two series expansions gives Verlet's algorithm for the positions as

$$r(t+\delta t) = 2r(t) - r(t-\delta t) + \frac{d^2r(t)}{dt^2}\delta t^2 + \mathscr{O}\left(\delta t^4\right) \tag{2.14}$$

Velocity Verlet Algorithm computes the positions velocities and accelerations of atoms at the same time.

$$r(t+\delta t) = r(t) + v(t)\delta t + \frac{1}{2}a(t)\delta t^2 + .. \tag{2.15}$$

$$v(t+\delta t) = v(t) + \frac{1}{2}\delta t[a(t) + a(t+\delta t)] + .. \tag{2.16}$$

The algorithm follows the steps,

- First update the velocities

$$v(t+\frac{\delta t}{2}) = v(t) + \frac{1}{2}a(t+\delta t) \tag{2.17}$$

- Update the positions

$$r(t+\delta t) = r(t) + v(t)(t+\frac{\delta t}{2})\delta t \tag{2.18}$$

- Evaluate the new forces, and thus accelerations
- Update velocities

$$v(t+\delta t) = v(t+\frac{\delta t}{2}) + \frac{1}{2}\delta t a(t+\delta t) \tag{2.19}$$

2.2.3 Periodic Boundary Conditions

One will mostly observe surface effects if simulations are conducted in some sort of container with walls that act as boundaries with which atoms collide when they attempt to leave the simulation region. In order to avoid surface effects, periodic boundary conditions are implemented. When an atom leaves the simulation box through a particular face , the particle reenters the simulation box by the opposite face as seen in Figure 2.6.

The particles have to interact with the replica boxes, in order to avoid a particle interacting with itself it is esential to have a cutoff distance smaller then the size of the box as seen in the Figure 2.7. The interactions between atoms of adjent replica are found thanks to the minimum image convention.

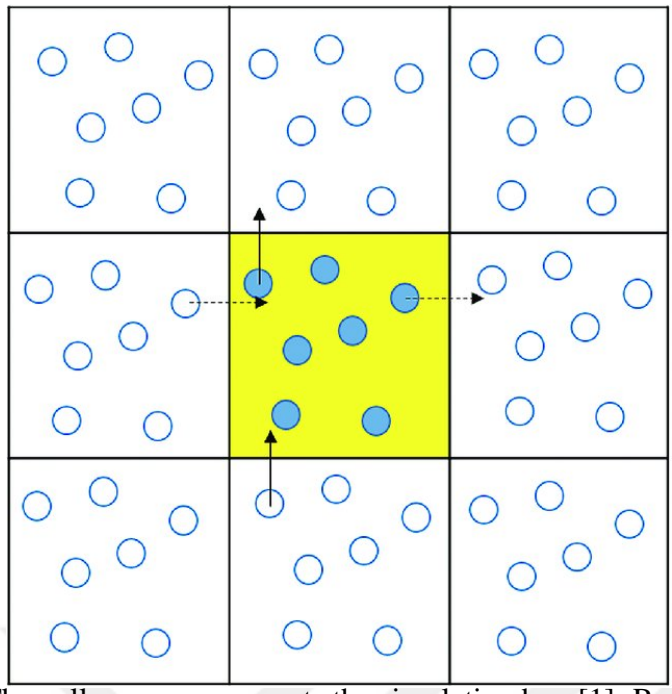

Figure 2.6 : The yellow area represents the simulation box [1]. Replication of the main cell in all directions.

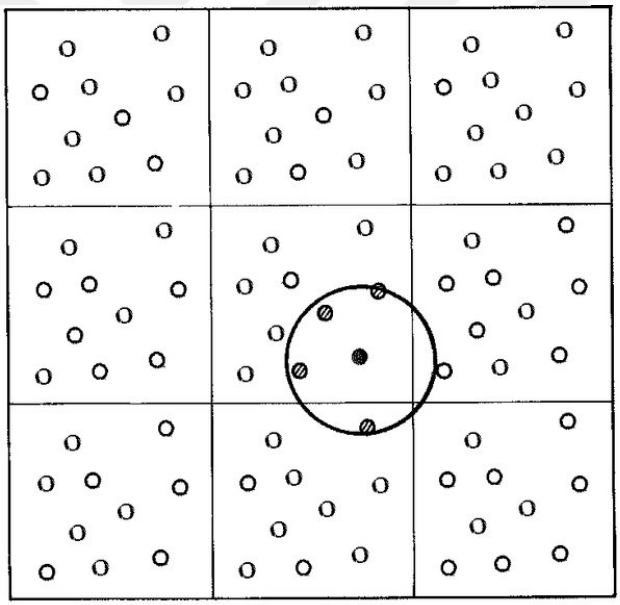

Figure 2.7 : The cut-off and the minimum image convention [2].

2.2.4 Neighbour list

In order to evaluate the non-bonded interactions, one has to calculate a double sum $\sum_{ij}$ over all the atoms. This computation scales as $\mathcal{O}(N^2)$ which is extremely ineffective. One can use neighbour list to have a more efficient code. Indeed, since the integration

time step is small, in a time step atoms move of a small distance, as a consequence for several time steps atoms stay close to each other, one could thus evaluate a list of neigthours and update it. The most effective neighbour list is called the cell linked list.

Cell subdivision offers a way to arrange the information about atom positions into a form that avoids most of the unnecessary work and speeds up the calculation. Cell subdivision is one of the techniques that reduces the computational effort from N^2 to $NlogN$. The simulation box is divided into cells with an edge slightly larger than the cutoff distance. Each cell has its own list [26]. This method is also much more efficient for large enough system [33]. Each particle interacts with the other particles that in the same cell list or in the neighbour cell list.

2.2.5 Testing the code

The trajectories we obtain by solving Newton's equations of motion correspond to the microcanonical ensamble. Thus the total energy E and momentum **P** are conserved.

These the constant of motion provide a way to ensure MD code works properly. We depisct in Figure 2.8, the kinetic, potential and total energy of a system as a function of a time. We see that while the energy fluctuates, it does not drift and furthermore the fluctiations are much smaller than the typical variations of the kinetic or potential energy. The total momentum of the bulk Lennard-Jones fluid is also conserved as seen in Figure 2.9.

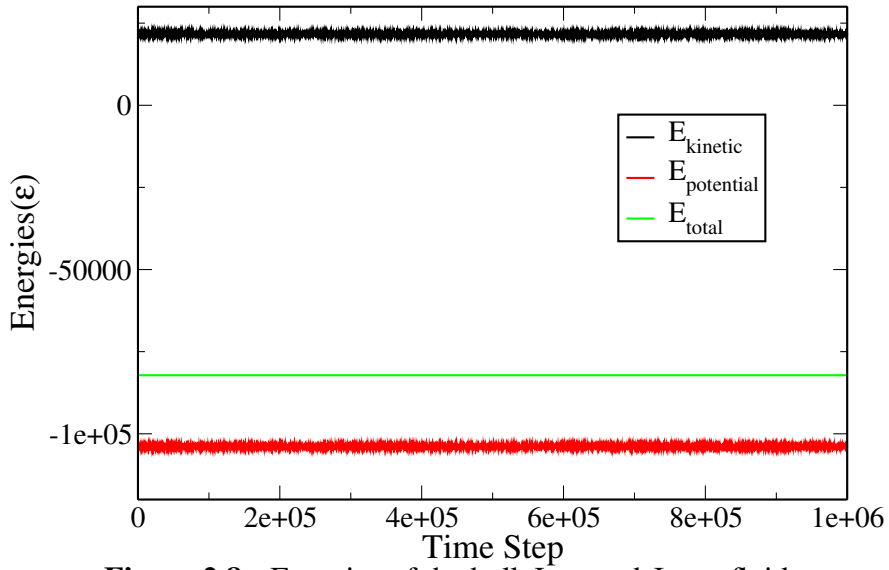

Figure 2.8 : Energies of the bulk Lennard-Jones fluid

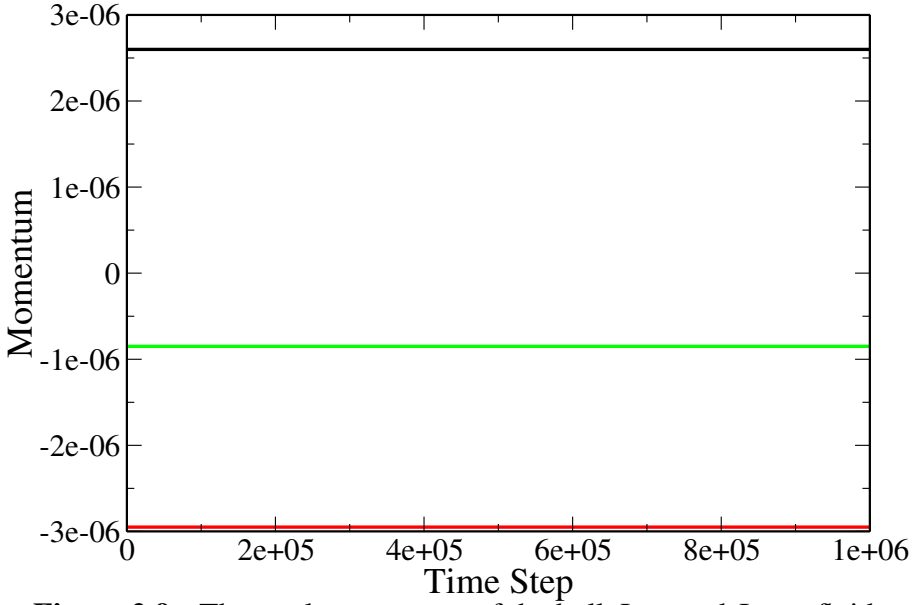

Figure 2.9 : The total momentum of the bulk Lennard-Jones fluid.

2.3 Thermal Conductivity

According to second law of thermodynamics, heat flow will occur from the hot environment to cold environment since the temperature difference is equilized by diffusion. This is quantified in terms of a heat flux. The dynamics of these energy exchanges are the main subject of heat transfer science [34].

The rate of heat transfer per unit area normal to the heat transfer direction is called heat flux and expressed as,

$$\mathbf{j}_\lambda = \frac{\dot{Q}}{A} \tag{2.20}$$

where $\dot{Q}$ is the heat transfer rate and A is the heat transfer area.

Thermal conductivity is a physical property of a material, that shows the material's ability to transfer heat. High thermal conductivity materials are employed as heat sinks, while low thermal conductivity materials are used as thermal insulators. Thermal conductivity λ can be described with Fourier's law where temperature gradient and heat flux are related. Fourier's law,

$$\mathbf{j}_\lambda = -\lambda \nabla T \tag{2.21}$$

where $\mathbf{j}_\lambda$ is heat flux, λ is thermal conductivity coefficient and ∇T is gradient of temperature. Thermal conductivity is quantified using the International Systems of Unit (SI Unit) of $[\lambda] = W/mK$.

2.3.1 Equilibrium method

In equilibrium molecular dynamics (EMD) method transport coefficients are evaluated by exploiting the fluctuation dissipation theorem. Green-Kubo relation gives mathematical expression for transport coefficients.

2.3.1.1 Green Kubo relation for thermal conductivity

The transported quantity is heat (energy), the associated Helfand moment is thus [35,36].

$$\mathbf{G}_\lambda = \frac{1}{V}\left[\sum_{i=1}^{N}(E_i - \langle E_i \rangle)\mathbf{r}_i + \sum_{\alpha=1}^{Nmol}\sum_{i_\alpha}^{N_p}(E_{i_\alpha} - \langle E_{i\alpha} \rangle)\mathbf{r}_{i_\alpha}\right] \tag{2.22}$$

where G is the centroid of transported quantitiy, E_i and E_{i_α} are the energy of fluid atoms and nanoparticle atoms respectively, where

$$E_i = \frac{1}{2}m\mathbf{v}_i^2 + \frac{1}{2}\sum_{j\neq i}^{N}\mathscr{V}_{LJ}(r_{i_\alpha j_\beta}) \tag{2.23}$$

$$E_{i_\alpha} = \frac{1}{2}m\mathbf{v}_{i_\alpha}^2 + \frac{1}{2}\sum_{j\neq i}^{N}\mathscr{V}_{SC}(r_{ij}) \tag{2.24}$$

where the $\mathbf{v}_i$ and m_i are velocity and mass of same fluid atom respectively and the $\mathbf{v}_{i_\alpha}$ and m_{i_α} are velocity and mass of same nanoparticle atom respectively. The thermal conductivity can be obtained from the mean square displacement of the Helfand moment,

$$\lambda = \frac{V}{k_b T^2}\lim_{t\to\infty}\frac{\langle[\mathbf{G}_\lambda(t) - \mathbf{G}_\lambda(0)]^2\rangle}{6t} \tag{2.25}$$

Using the property relating MSD to time auto-correlation function we can write

$$\lim_{t\to\infty}\frac{\langle[\mathbf{G}_\lambda(t)-\mathbf{G}_\lambda(0)]^2\rangle}{6t}=\int_0^\infty d\tau\langle\mathbf{j}_\lambda(\tau)\mathbf{j}_\lambda(0)\rangle \tag{2.26}$$

where the heat flux is the time derivative of the Helfand moment,

$$\mathbf{j}_\lambda=\frac{d\mathbf{G}_\lambda}{dt} \tag{2.27}$$

Green-Kubo relation, the thermal conductivity coefficient λ is based on the integration of the time autocorrelation function of the heat current J_λ.

The microscopic heat current can be expressed as:

$$\mathbf{j}_{LL}=\frac{1}{V}\left[\sum_i(E_i-\langle E_i\rangle)\mathbf{v}_i+\frac{1}{2}\sum_{i<j}\mathbf{r}_{ij}[\mathbf{F}_{LL}(\mathbf{r}_{ij}).(\mathbf{v}_i+\mathbf{v}_j)]\right] \tag{2.28}$$

$$\mathbf{j}_{NN}=\frac{1}{V}\left[\sum_\alpha\sum_{i_\alpha}(E_{i_\alpha}-\langle E_{i_\alpha}\rangle)\mathbf{v}_{i_\alpha}+\frac{1}{2}\sum_{i_\alpha<j_\beta}\mathbf{r}_{i_\alpha j_\beta}[\mathbf{F}_{NN}(\mathbf{r}_{i_\alpha j_\beta}).(\mathbf{v}_{i_\alpha}+\mathbf{v}_{j_\beta})]\right] \tag{2.29}$$

$$\mathbf{j}_{LN}=\frac{1}{V}\frac{1}{2}\sum_i\sum_\alpha\sum_{i_\alpha}\mathbf{r}_{ii_\alpha}[\mathbf{F}_{LN}(\mathbf{r}_{ii_\alpha}).(\mathbf{v}_i+\mathbf{v}_{i_\alpha})] \tag{2.30}$$

$$\mathbf{j}_{SC}=\frac{1}{V}\frac{1}{2}\sum_\alpha^{Nmol}\sum_{i_\alpha<j_\alpha}^{Np}\mathbf{r}_{i_\alpha j_\alpha}[\mathbf{F}_{SC}(r_{i_\alpha j_\alpha}).(\mathbf{v}_{i_\alpha}+\mathbf{v}_{j_\alpha})] \tag{2.31}$$

$$\mathbf{j}_\lambda=\mathbf{j}_{LL}+\mathbf{j}_{NN}+\mathbf{j}_{LN}+\mathbf{j}_{SC} \tag{2.32}$$

where $\mathbf{j}_{LL}$, $\mathbf{j}_{NN}$, $\mathbf{j}_{LN}$ and $\mathbf{j}_{SC}$ is the microscopic heat current between fluid atoms, between atoms of nanoparticle, between fluid and atoms of nanoparticle, between nanoparticles respectively.

Thus the termal conductivity as follows,

$$\lambda=\frac{V}{3k_bT^2}\int_0^\infty d\tau\langle\mathbf{j}_\lambda(\tau)\mathbf{j}_\lambda(0)\rangle \tag{2.33}$$

2.3.2 Reverse non-equilibrium method

The finite-size effects by a finite simulation cell are a significant difference between the non equilibrium molecular dynamics (NEMD) and EMD methods [37]. When periodic boundary conditions are used in the EMD technique, one can typically achieve size-independent thermal conductivity using a small simulation cell; nevertheless, the cell size does not exactly match the size of a real sample as in an actual measurement setup. The simulation cell length (in the transport direction) for the NEMD approach is meant to correspond to the sample length used in actual investigations. Therefore, heat transport is largely ballistic (transporting without scattering) when the cell length is shorter than the overall phonon mean free route, and the thermal conductivity should be lower than that in an infinitely long system [38]. Boundary-driven NEMD is based on the principle of allowing external forces to interact with a system's limits in an experimental setting. These techniques fall into two categories when it comes to thermal processes.

A temperature gradient is applied to the system in the first group, which is a direct method, and the resulting flux is then measured. Thermal walls [39] or the use of a thermostat like a Nose thermostat to keep some areas hotter than others can create temperature gradients.

The second group uses the reverse non equilibrium (RNEMD) method, which imposes a heat flux on the system and calculates the ensuing temperature gradient. Technically, this is accomplished by adding energy to the heated region and removing energy from the cool region [40]–[43].

2.3.2.1 Velocity exchange method

Simulation box is divided into N slabs in z direction. Figure 2.10 shows the simuation box according to velocity exchange method.

Kinetic temperature for each slab can be calculated as

$$T_k = \frac{1}{3n_k k_b} \sum_{i \varepsilon k}^{n_k} m_i \mathbf{v}_i^2 \tag{2.34}$$

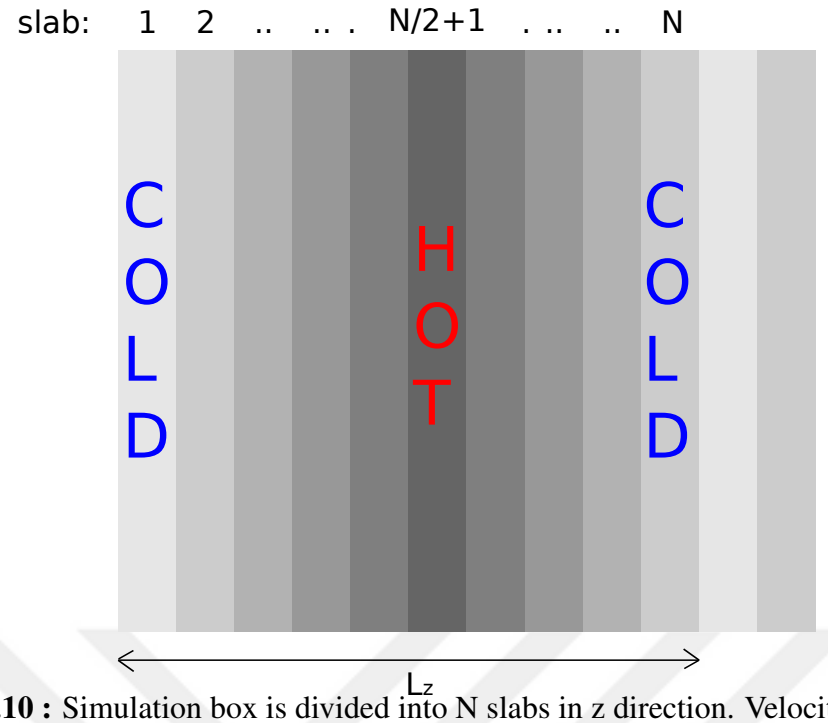

Figure 2.10 : Simulation box is divided into N slabs in z direction. Velocities of hot atoms in Slab 1 and cold atoms in Slab N/2+1 are exchanged.

where k is number of slab.

Slab "1" is chosen as cool slab, Slab "N/2+1" is chosen as hot slab as shown in Figure 3.1. Since atoms have same mass, to impose heat flux velocity vectors of the hottest atom in the cool slab and the coldest atom in the hot slab are exchanged.

Thermal conductivity,

$$\lambda = -\frac{\sum_{transfers} \frac{m}{2}(\mathbf{v}_h^2 - \mathbf{v}_c^2)}{2tL_xL_y\langle \partial T/\partial z \rangle} \tag{2.35}$$

where $\mathbf{v}_h$ and $\mathbf{v}_c$ are the velocity of hot and cold atoms respectively. Since the mass of hot and cold atoms are same, after exchanging velocities, energy and total momentum of the system will be conserved.

2.3.2.2 Dual thermostat method

Simulation box is divided into N slabs in z direction. Figure 2.11 shows the simuation box according to Dual Thermostat method.

In dual-thermostat method, berendsen thermostats are placed in simulation box in slab "1" and in slab "N/2+1" to maintain temperatures of slabs to desired temperature.

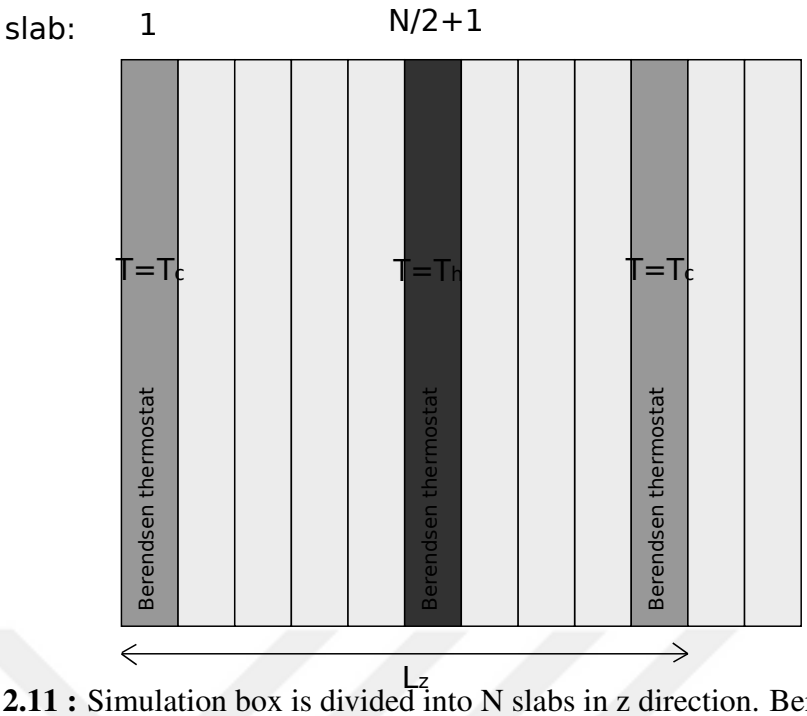

Figure 2.11 : Simulation box is divided into N slabs in z direction. Berendsen thermostats are placed in slab "1" and in slab "N/2+1".

Berendsen thermostat

$$\mathbf{v}^{'} = \mathbf{v}\sqrt{1+\frac{1}{n}\left(\frac{T_0}{T(t)}-1\right)} \tag{2.36}$$

where n is a relaxation time and,

$$T(t) = \frac{2E_k(t)}{3N} \tag{2.37}$$

The temperature of the slab at time t. Since the aim is to impose a temperature difference dT, we define the temperature of slab 1 as $T_c = T_0 - 0.5 * dT$, and the one of slab N/2+1 as $T_h = T_0 + 0.5 * dT$. Where T_0 is the average temperature of the box.

The Berendsen thermostat do not conserve energy, however the change in total energy can be written as,

$$\langle \Delta E_{total} \rangle = \langle \Delta E_H \rangle + \langle \Delta E_C \rangle + \langle \Delta E_{error} \rangle \tag{2.38}$$

ΔE_C and ΔE_H are the energy change due to velocity scaling by the Berendsen thermostat. ΔE_{error} is the change due to numerical errors per MD step. On average the total energy is conserved.

Kinetic energy of each slab,

$$E_i^K = \frac{1}{2}\sum_{j\varepsilon i} m_j \mathbf{v}_j^2 \tag{2.39}$$

where i is number of slab.

Thermal conductivity becomes,

$$\lambda = \frac{1}{2A}\frac{\langle|\Delta E_i/\Delta t|\rangle}{\langle|dT(z)/dz|\rangle} \tag{2.40}$$

where A is cross section area that is perpendicular to the z direction. Since we set the temperature of first slab and the middle slab to desired temperature, by dual thermostat method energy and total momentum will not be conserved.

3. RESULTS

In this section we evaluate the thermal conductivity of the nanofluids with different volume fractions using EMD and the two rNEMD methods.

3.1 Green Kubo Result for the Base Lennard Jones Fluid

The heat current $\mathbf{j}_\lambda$ of base fluid is computed by using equation 2.25. Heat current vector in all directions are showed in Figure 3.1 for base fluid.

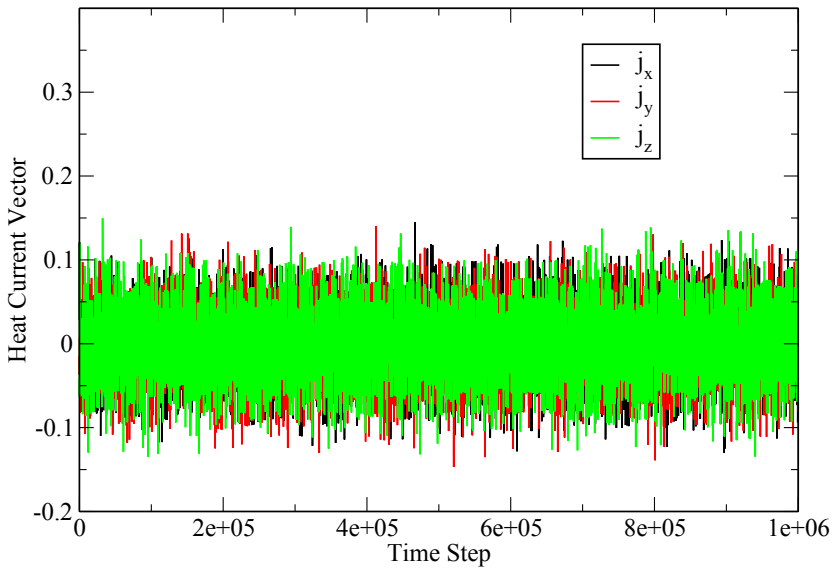

Figure 3.1 : Heat current in three directions for base fluid.

Figure 3.2(a) shows the heat current auto correlation function while Figure 3.2(b) shows the thermal conductivity, which is calculated as the time integral of the heat current auto correlation function. The thermal conductivity coefficient is found as approximately $\lambda = 6.9\frac{k_B}{\sigma^2}\sqrt{\frac{\varepsilon}{m}}$.

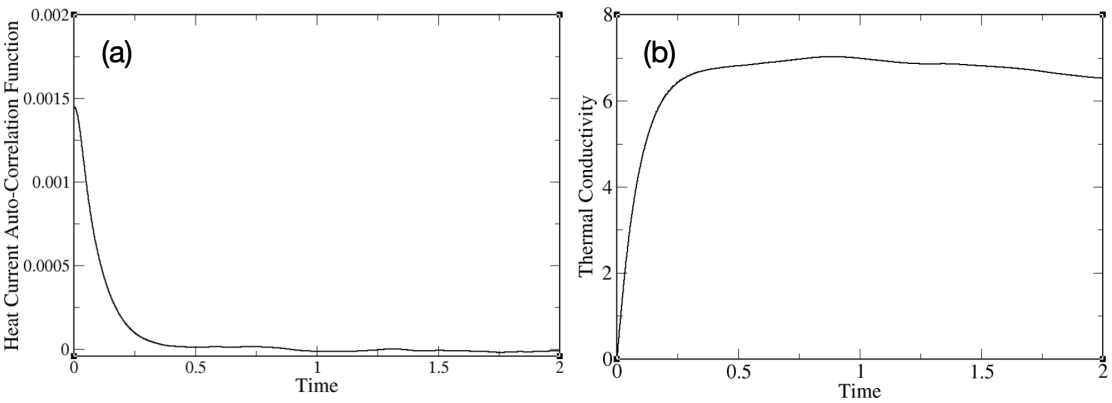

Figure 3.2 : (a) Heat current auto-correlation function (b) Thermal conductivity of the base fluid.

Then, we examined the thermal conductivity of base fluid at different number of atoms. Figure 3.3(a) shows the heat current auto correlation function while Figure 3.3(b) shows the thermal conductivity of base fluid at different number of atoms.

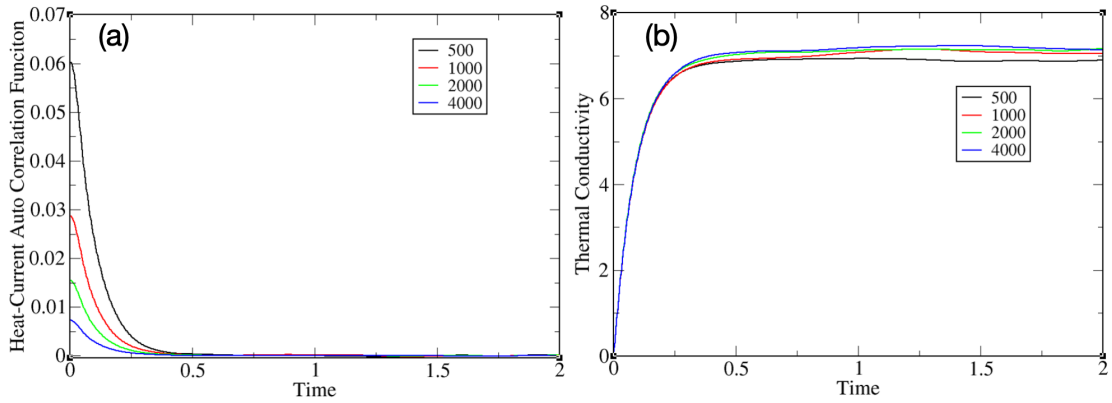

Figure 3.3 : (a) Heat current auto-correlation function (b) Thermal conductivity of the base fluid at different number of atoms.

Figure 3.4 shows the thermal conductivity of base fluid at different number of atoms from 500 to 4000. It is clearly seen from the Figure 3.4 that with the increase of number of atoms the thermal conductivity increased.

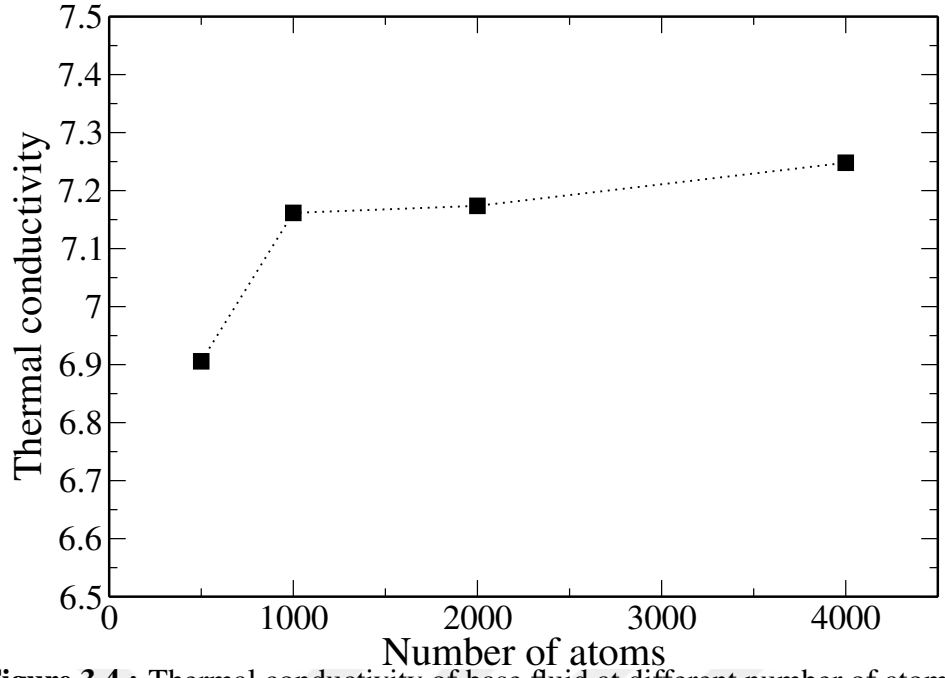

Figure 3.4 : Thermal conductivity of base fluid at different number of atoms.

3.2 Reverse Non-Equilibrium Methods

3.2.1 Velocity exchange method

The thermal conductivity within the velocity exchange method is determined as,

$$\lambda = -\frac{\sum_{transfers} \frac{m}{2}(v_h^2 - v_c^2)}{2tL_xL_y\langle \partial T/\partial z \rangle} \tag{3.1}$$

The numerator is evaluated during the simulation, the velocities of the fastest atom in the cold slab is exchanged with the velocity of the slowest atom in the hot slab every W time steps. The change in kinetic energy is then evaluated and added to the previous exhcanges. We carry out three sets of simulations with W=80,100 and 120.

We depict in Figure 3.1 the temperature profile. We use the fact that the system is periodic and take the average of the slope calculated on both sides of the temperature profile. Heat flux results are given in Table 3.1.

Combining the differences of kinetic energies and the temperature gradients we evaluate the thermal conductivity for different volume fractions and values of W. The results are depicted in Figure 3.5.

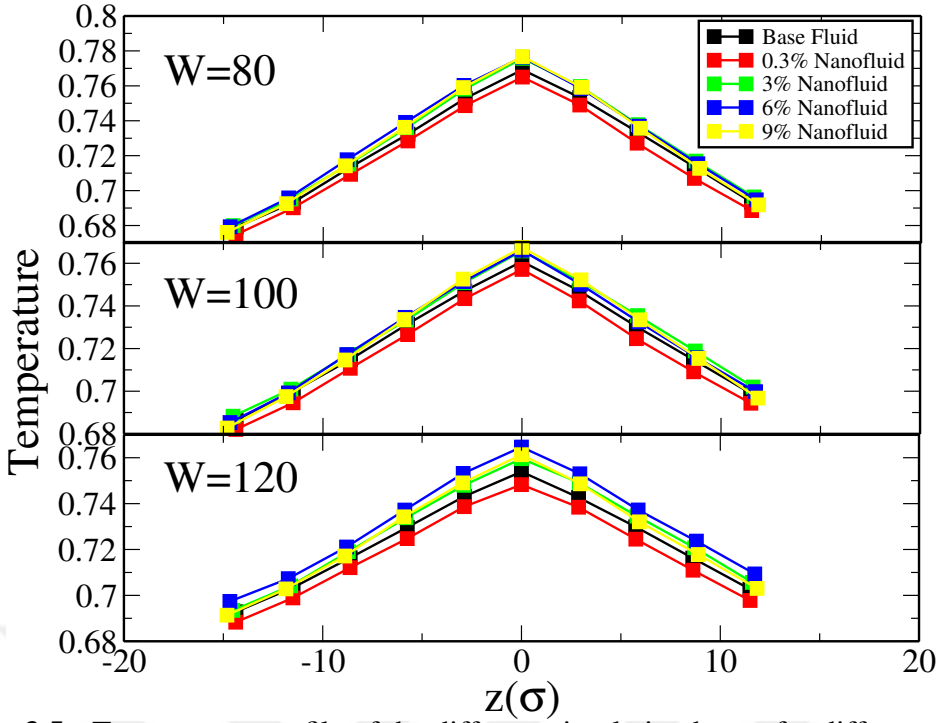

Figure 3.5 : Temperature profile of the different simulation boxes for different values of W.

Table 3.1 : Heat flux according to W.

φ	80	100	120
0	0.0485	0.0393	0.0330
0.3	0.0481	0.0390	0.0328
3	0.0474	0.0384	0.0323
6	0.0464	0.0376	0.0319
9	0.0451	0.0367	0.0309

We depict in Figure 3.6 the thermal conductivity for three different values of W. We observe that the three different curves give similar results, surprisingly in each case the thermal conductivity decreases with volume fraction, except at very low volume fraction for the exchange rate W=120 where a slight increase is observed.

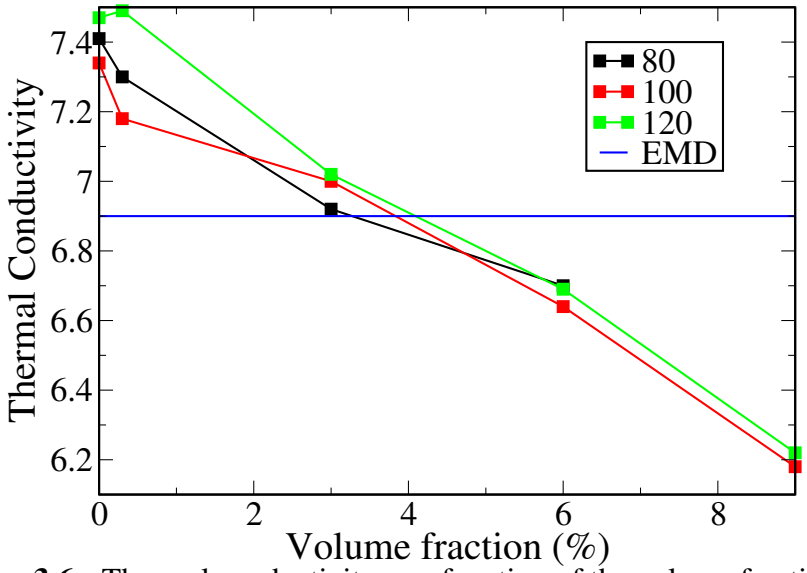

Figure 3.6 : Thermal conductivity as a function of the volume fraction of nanoparticles for different values of W.

3.2.2 Dual-thermostat method

The thermal conductivity within the dual thermostat method is determined as,

$$\lambda = \frac{1}{2A} \frac{\langle |\Delta E_i / \Delta t| \rangle}{\langle |dT(z)/dz| \rangle} \tag{3.2}$$

Temperature of first slab set to $T_c = T_0 - 0.5 * dT$, and temperature of the one of slab in the middle is set to $T_h = T_0 + 0.5 * dT$. Where T_0 is the average temperature of the box, thus we have the same temperature profile for each volume fractions. Figure 3.7 shows the temperature profiles for a relaxation time $n = 100$ and $n = 500$ and temperature difference dT=0.05. We use the fact that the system is periodic and take the average of the slope. Heat flux results are given in Table 3.2.

Table 3.2 : Heat flux according to n.

φ	100	500
0	0.0248	0.0208
0.3	0.0250	0.0209
3	0.0230	0.0194
6	0.0221	0.0191
9	0.0210	0.0175

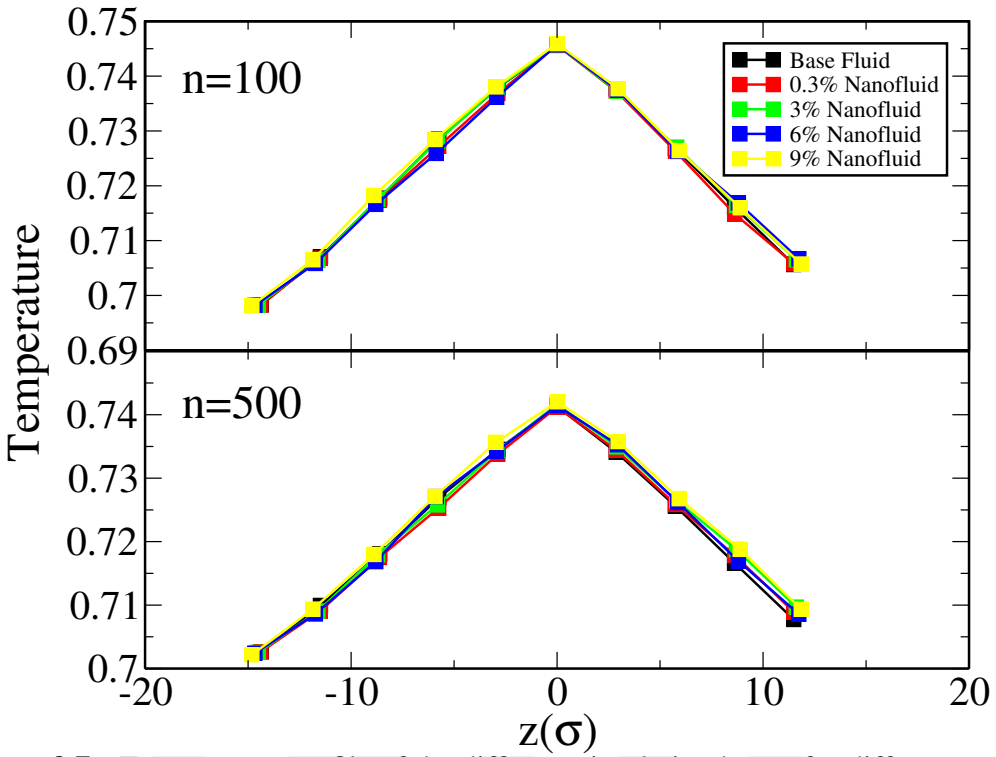

Figure 3.7 : Temperature profile of the different simulation boxes for different values of n.

We evaluate the thermal conductivity for different volume fractions and values of n. The results are depicted in Figure 3.8. As for the velocity exchange method we observe a systematic decrease of the thermal conductivity except at very low volume fractions where a slight increase occurs.

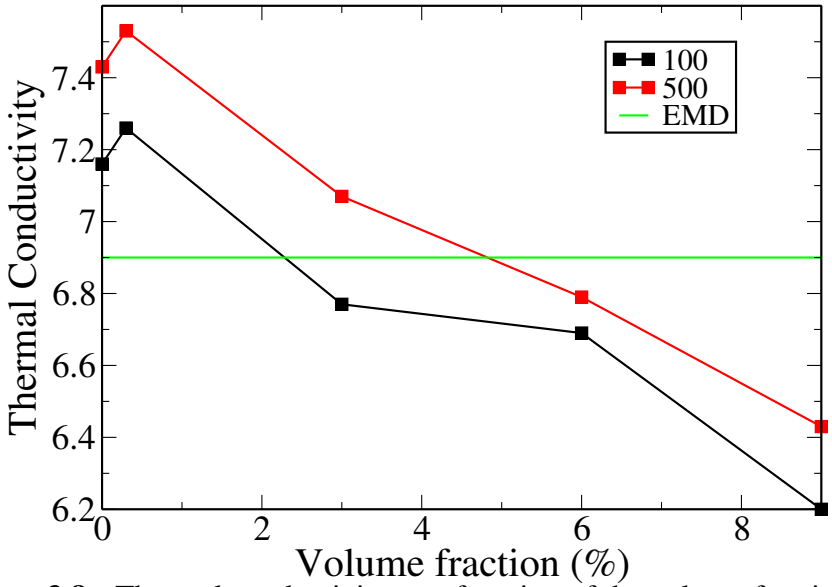

Figure 3.8 : Thermal conductivity as a function of the volume fraction of nanoparticles for different values of n.

3.3 Equilibrium Method

The heat current vector $\mathbf{j}_\lambda$ computed by using equation 3.9. The heat current in all directions are showed in Figure 3.9 for 0.3% nanofluid and 9% nanofluid.

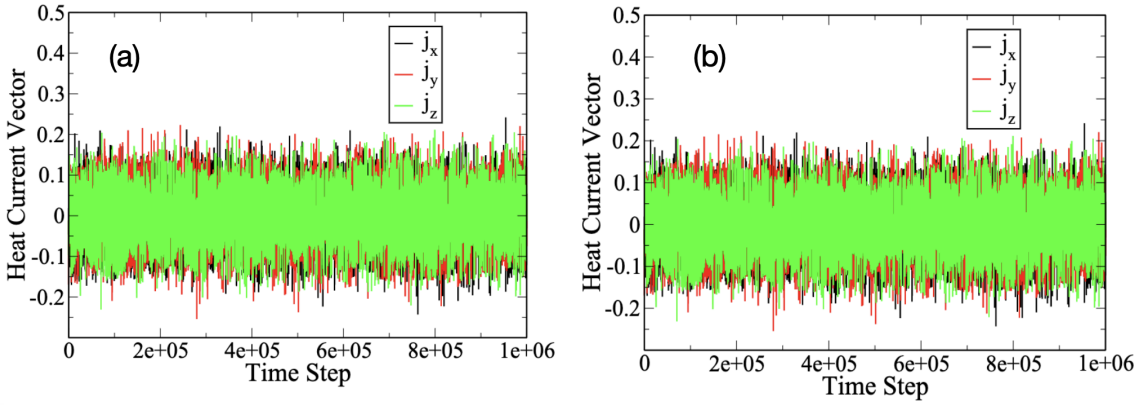

Figure 3.9 : Heat current in three directions for (a) 0.3% Nanofluid (b) 9% Nanofluid

Figure 3.10(a) shows the heat current auto correlation function while Figure 3.10(b) shows the thermal conductivity, which is calculated as the time integral of the heat current auto correlation function. The thermal conductivity coefficient is found approximately $7.6\frac{k_B}{\sigma^2}\sqrt{\frac{\varepsilon}{m}}$ for 0.3% nanofluid, $10\frac{k_B}{\sigma^2}\sqrt{\frac{\varepsilon}{m}}$ for 9% nanofluid.

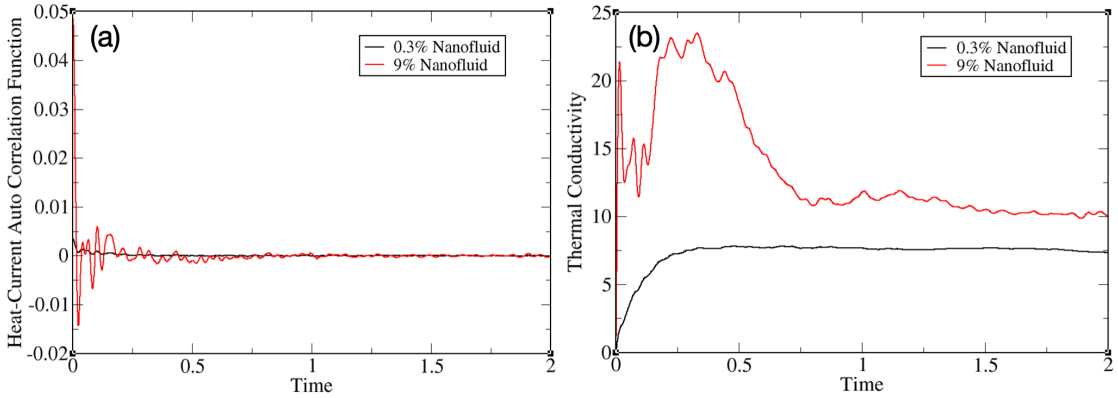

Figure 3.10 : (a) Decay of the heat current auto-correlation function and (b) integral of the heat current auto-correlation function of 0.3% Nanofluid and 9% Nanofluid.

We evaluated the thermal conductivity of nanofluid as a function of volume fraction by EMD and rNEMD methods. Different values of n and W should be aveluated to make sure. However, the results of rNEMD calculations are not in agreement with EMD results. In rNEMD method we observed small increase at the thermal conductivity only at 0.3% nanofluid. For EMD calculations we found enhancement in 0.3% nanofluid and 9% nanofluid.

4. CONCLUSION

In this thesis, we calculated the thermal conductivity of nanofluids with various volume fractions with molecular dynamics simulations. Two different reverse non-equilibrium molecular dynamics methods, namely are dual thermostat method and velocity exchange method are employed to calculate the thermal conductivity of nanofluids with metallic nanoparticles. Also, to check the consistency of our results, equilibrium molecular dynamics simulations are carried out. For the fluid-fluid, fluid-nanoparticle, and nanoparticle-nanoparticle interactions the Lennard-Jones potential is used and for the interatomic interactions in the nanoparticles we used the quantum corrected Sutton-Chen (Q-SC) many body potential.

For the rNEMD methods, the results showed that there is a decrease in thermal conductivity of nanofluids with metallic nanoparticles at higher volume fractions. In the velocity exchange method, with three different W values, the thermal conductivity decreased however when W is taken as 120 thermal conductivity increased slightly at the volume of 0.3% nanoparticle, so it is not consistent. However, in the dual thermostat method thermal conductivities have same pattern for two different relaxation times, τ, values, and thermal conductivity slightly increased for a volume fraction of 0.3% nanoparticle then decreased which is more acceptable.

Consequently, in order to check the consistency of our results of the thermal conductivity by rNEMD methods and to find a reasonable explanation for the decrease in the thermal conductivity at higher volume fractions, we performed equilibrium molecular dynamics method and the results of EMD method is not consistent with the rNEMD methods. Maybe the average atomic energies are incorrectly defined, which affects the thermal conductivity of the nanofluid. When the average atom energies of the nanoparticles were not accurately calculated that can led to significant increase in thermal conductivity. Thus, we should perform well established equilibrium molecular

dynamics method. Additionally, different sizes and shapes of metallic nanoparticles should be studied.

REFERENCES

[1] **Katiyar, R.S. and Jha, P.K.** (2018). *Molecular simulations in drug delivery: Opportunities and challenges*.

[2] **Brasiello, A.**, **Grizzuti, N. and Milano, G.** (2006). *Molecular dynamics of triglycerides: atomistic and coarse-grained approaches Poisson-Kac processes View project Modeling Bio Nanomaterials Interfaces View project*, `https://www.researchgate.net/publication/228387451`.

[3] **Alder, B.J. and Wainwright, T.E.** (1959). Studies in molecular dynamics. I. General method, *The Journal of Chemical Physics*, *31*.

[4] **Vakili-Nezhaad, G.R.**, **Al-Wadhahi, M.**, **Gujarathi, A.M.**, **Al-Maamari, R. and Mohammadi, M.** (2019). Molecular dynamics simulation of water–graphene nanofluid, *SN Applied Sciences*, *1*.

[5] **Salomon-Ferrer, R.**, **Götz, A.W.**, **Poole, D.**, **Le Grand, S. and Walker, R.C.** (2013). Routine Microsecond Molecular Dynamics Simulations with AMBER on GPUs. 2. Explicit Solvent Particle Mesh Ewald, *Journal of Chemical Theory and Computation*, *9*(9), 3878–3888, pMID: 26592383.

[6] **Nejatolahi, M.**, **Golneshan, A.A.**, **Kamali, R. and Sabbaghi, S.** (2021). Nonequilibrium versus equilibrium molecular dynamics for calculating the thermal conductivity of nanofluids, *Journal of Thermal Analysis and Calorimetry*, *144*.

[7] **Müller-Plathe, F.** (1997). A simple nonequilibrium molecular dynamics method for calculating the thermal conductivity, *Journal of Chemical Physics*, *106*.

[8] **Terao, T.**, **Lussetti, E. and Müller-Plathe, F.** (2007). Nonequilibrium molecular dynamics methods for computing the thermal conductivity: Application to amorphous polymers, *Physical Review E - Statistical, Nonlinear, and Soft Matter Physics*, *75*.

[9] **Wen, Y.H.**, **Fang, H.**, **Zhu, Z. and Sun, S.G.** (2009). Molecular dynamics investigation of shape effects on thermal characteristics of platinum nanoparticles, *Physics Letters, Section A: General, Atomic and Solid State Physics*, *373*.

[10] **Topal, I. and Servantie, J.** (2019). Molecular dynamics study of the thermal conductivity in nanofluids, *Chemical Physics*, *516*.

[11] **Khedkar, R.S.**, **Sai, K.A.**, **Sonawane, S.S.**, **Wasewar, K. and Umre, S.S.** (2013). Thermo physical characterization of paraffin based Fe3O 4 nanofluids, volume 51.

[12] **Sankar, N.**, **Mathew, N. and Sobhan, C.B.** (2008). Molecular dynamics modeling of thermal conductivity enhancement in metal nanoparticle suspensions, *International Communications in Heat and Mass Transfer*, *35*.

[13] **Choi, S.U. and Eastman, J.** (1995). Enhancing thermal conductivity of fluids with nanoparticles, developments and applications of non-newtonian flows, *ASME, New York*, *38*.

[14] **Maxwell, J.C.** (1881). *A Treatise on Electricity and Magnetism*, volume 1, 2nd. edition.

[15] **Masuda, H.**, **Ebata, A.**, **Teramae, K. and Hishinuma, N.** (1993). Alteration of Thermal Conductivity and Viscosity of Liquid by Dispersing Ultra-Fine Particles. Dispersion of Al2O3, SiO2 and TiO2 Ultra-Fine Particles., *Netsu Bussei*, *7*.

[16] **Puliti, G.**, **Paolucci, S. and Sen, M.** (2012). Nanofluids and Their Properties, *Applied Mechanics Reviews*, *64*(3), https://doi.org/10.1115/1.4005492, 030803, https://asmedigitalcollection.asme.org/appliedmechanicsreviews/article-pdf/64/3/030803/6072907/amr_64_3_030803.pdf.

[17] **Younes, H.**, **Mao, M.**, **Murshed, S.S.**, **Lou, D.**, **Hong, H. and Peterson, G.** (2022). Nanofluids: Key parameters to enhance thermal conductivity and its applications, *Applied Thermal Engineering*, *207*, 118202, https://linkinghub.elsevier.com/retrieve/pii/S1359431122001648.

[18] **Eastman, J.A.**, **Choi, S.U.**, **Li, S.**, **Yu, W. and Thompson, L.J.** (2001). Anomalously increased effective thermal conductivities of ethylene glycol-based nanofluids containing copper nanoparticles, *Applied Physics Letters*, *78*.

[19] **Patel, H.E.**, **Das, S.K.**, **Sundararajan, T.**, **Nair, A.S.**, **George, B. and Pradeep, T.** (2003). Thermal conductivities of naked and monolayer protected metal nanoparticle based nanofluids: Manifestation of anomalous enhancement and chemical effects, *Applied Physics Letters*, *83*.

[20] **Bahiraei, M.** (2016). *Particle migration in nanofluids: A critical review*.

[21] **Mohebbi, A.** (2012). Prediction of specific heat and thermal conductivity of nanofluids by a combined equilibrium and non-equilibrium molecular dynamics simulation, *Journal of Molecular Liquids*, *175*.

[22] **Murshed, S.M.**, **Leong, K.C. and Yang, C.** (2005). Enhanced thermal conductivity of TiO2 - Water based nanofluids, *International Journal of Thermal Sciences*, *44*.

[23] **Kim, S.H.**, **Choi, S.R. and Kim, D.** (2007). Thermal conductivity of metal-oxide nanofluids: Particle size dependence and effect of laser irradiation, *Journal of Heat Transfer*, *129*.

[24] **Jones, J.** (1924). On the determination of molecular fields.—I. From the variation of the viscosity of a gas with temperature, *Proceedings of the Royal Society of London. Series A, Containing Papers of a Mathematical and Physical Character*, *106*, 441–462.

[25] **Lennard-Jones, J.E.** (1931). Cohesion, *Proceedings of the Physical Society*, *43*.

[26] **Rapaport, D.** (2004). *The Art of Molecular Dynamics Simulation*, 2nd. edition.

[27] **Fernández, G.A.**, **Vrabec, J. and Hasse, H.** (2004). A molecular simulation study of shear and bulk viscosity and thermal conductivity of simple real fluids, *Fluid Phase Equilibria*, *221*.

[28] **Topal, I.** (2017). *MOLECULAR DYNAMICS STUDY OF THE THERMAL CONDUCTIVITY IN NANOFLUIDS*.

[29] **Daw, M.S.**, **Foiles, S.M. and Baskes, M.I.** (1993). *The embedded-atom method: a review of theory and applications*.

[30] **Daw, M.S. and Baskes, M.I.** (1983). Semiempirical, quantum mechanical calculation of hydrogen embrittlement in metals, *Physical Review Letters*, *50*.

[31] **Daw, M.S. and Baskes, M.I.** (1984). Embedded-atom method: Derivation and application to impurities, surfaces, and other defects in metals, *Physical Review B*, *29*.

[32] **Kimura, Y.**, **Qi, Y.**, **Ggn, T.C. and III, W.A.G.** (1998). The Quantum Sutton-Chen Many-Body Potential for Properties of fcc Metals, *California Institute of Technology*.

[33] **Haile, J.M.** (1992). Molecular Dynamics Simulation Elementary Methods.

[34] **Cengel, Y.A. and Ghajar, A.J.** (2014). *Heat and Mass Transfer, Fundamentals Application, Fifth Edition in SI Units*, volume5th.

[35] **Green, M.S.** (1960). Comment on a paper of mori on time-correlation expressions for transport properties, *Physical Review*, *119*.

[36] **Kubo, R.** (1957). Statistical'Mechanical Theory of Irreversible Processes. I. General Theory and Simple Applications to Magnetic and Conduction Problems, *Journal of the Physical Society of Japan*, *12*.

[37] **Wang, Z. and Ruan, X.** (2017). On the domain size effect of thermal conductivities from equilibrium and nonequilibrium molecular dynamics simulations, *Journal of Applied Physics*, *121*.

[38] **Dong, H.**, **Fan, Z.**, **Shi, L.**, **Harju, A. and Ala-Nissila, T.** (2018). Equivalence of the equilibrium and the nonequilibrium molecular dynamics methods for thermal conductivity calculations: From bulk to nanowire silicon, *Physical Review B*, *97*.

[39] **Tenenbaum, A.**, **Ciccotti, G. and Gallico, R.** (1982). Stationary nonequilibrium states by molecular dynamics. Fourier's law, *Phys. Rev. A*, *25*, 2778–2787, https://link.aps.org/doi/10.1103/PhysRevA.25.2778.

[40] **Kincaid, J.**, **Li, X. and Hafskjold, B.** (1992). Nonequilibrium molecular dynamics calculation of the thermal diffusion factor, *Fluid Phase Equilibria*, *76*, 113–121, https://www.sciencedirect.com/science/article/pii/037838129285081I.

[41] **Hafskjold, B.**, **Ikeshoji, T. and Ratkje, S.K.** (1993). On the molecular mechanism of thermal diffusion in liquids, *Molecular Physics*, *80*(6), 1389–1412.

[42] **Ikeshoji, T. and Hafskjold, B.** (1994). Non-equilibrium molecular dynamics calculation of heat conduction in liquid and through liquid-gas interface, *Molecular Physics*, *81*(2), 251–261.

[43] **Baranyai, A.** (1996). Heat flow studies for large temperature gradients by molecular dynamics simulation, *Phys. Rev. E*, *54*, 6911–6917, https://link.aps.org/doi/10.1103/PhysRevE.54.6911.

APPENDICES

APPENDIX A : Heat Current Vector

APPENDIX A : Heat Current Vector

$$\mathbf{j}_\lambda = \frac{d\mathbf{G}}{dt} \tag{A.1}$$

$$\mathbf{G} = \sum_i (E_i - \langle E_i \rangle)\mathbf{r}_i + \sum_{\alpha=1}^{N_{mol}} \sum_{i_\alpha=1}^{N_p} (E_{i_\alpha} - \langle E_{i_\alpha} \rangle)\mathbf{r}_{i_\alpha} \tag{A.2}$$

$$\frac{d\mathbf{G}_L}{dt} = \sum_i (E_i - \langle E_i \rangle)\mathbf{v}_i + \sum_i \mathbf{r}_i \frac{d\mathbf{E}_i}{dt} \tag{A.3}$$

where

$$E_i = \frac{1}{2} m \mathbf{v}_i^2 + \frac{1}{2} \sum_{j=1}^{N_L} V_{LL}(r) + \frac{1}{2} \sum_{\alpha=1}^{N_{mol}} \sum_{i_\alpha=1}^{N_p} V_{LN}(r) \tag{A.4}$$

$$\frac{d\mathbf{G}_L}{dt} = \sum_{i=1}^{N_L} (E_i - \langle E_i \rangle)\mathbf{v}_i + \frac{1}{2} \sum_{i=1}^{N_L} \sum_{j=1}^{N_L} \mathbf{r}_i [\mathbf{F}_{LL}(r).(\mathbf{v}_i + \mathbf{v}_j)] + \frac{1}{2} \sum_{i=1}^{N_L} \sum_{\alpha=1}^{N_{mol}} \sum_{i_\alpha=1}^{N_p} \mathbf{r}_i [F_{LN}(r).(\mathbf{v}_i + \mathbf{v}_{i_\alpha})] \tag{A.5}$$

$$\frac{d\mathbf{G}_N}{dt} = \sum_{\alpha=1}^{N_{mol}} \sum_{i_\alpha=1}^{N_p} (E_{i_\alpha} - \langle E_{i_\alpha} \rangle)\mathbf{v}_{i_\alpha} + \sum_{\alpha=1}^{N_{mol}} \sum_{i_\alpha=1}^{N_p} \mathbf{r}_{i_\alpha} \frac{dE_{i_\alpha}}{dt} \tag{A.6}$$

$$\mathbf{j}_L = \sum_i (E_i - \langle E_i \rangle)\mathbf{v}_i + \frac{1}{2} \sum_{i<j}^{N_L} \mathbf{r}_{ij} [F_{LL}(r).(\mathbf{v}_i + \mathbf{v}_j)] + \frac{1}{2} \sum\sum\sum \mathbf{r}_{ii_\alpha} [F_{LN}(r).(\mathbf{v}_i + \mathbf{v}_{i_\alpha})] + \frac{1}{2} \sum\sum\sum \mathbf{r}_{i_\alpha} [F_{LN}(r).(\mathbf{v}_i + \mathbf{v}_{i_\alpha})] \tag{A.7}$$

$$\mathbf{j}_{LL} = \frac{1}{V} \sum_i (E_i - \langle E_i \rangle)\mathbf{v}_i + \frac{1}{2} \sum_{i<j} \mathbf{r}_{ij} [\mathbf{F}_{LL}(\mathbf{r}_{ij}).(\mathbf{v}_i + \mathbf{v}_j)] \tag{A.8}$$

$$\mathbf{j}_{NN} = \frac{1}{V} \sum_\alpha \sum_{i_\alpha} (E_{i_\alpha} - \langle E_{i_\alpha} \rangle)\mathbf{v}_{i_\alpha} + \frac{1}{2} \sum_{i_\alpha < j_\beta} \mathbf{r}_{i_\alpha j_\beta} [\mathbf{F}_{NN}(\mathbf{r}_{i_\alpha j_\beta}).(\mathbf{v}_{i_\alpha} + \mathbf{v}_{j_\beta})] \tag{A.9}$$

$$\mathbf{j}_{LN} = \frac{1}{V} \frac{1}{2} \sum_i \sum_\alpha \sum_{i_\alpha} \mathbf{r}_{ii_\alpha} [\mathbf{F}_{LN}(\mathbf{r}_{ii_\alpha}).(\mathbf{v}_i + \mathbf{v}_{i_\alpha}) \tag{A.10}$$

$$V_{sc} = \frac{1}{2}\sum_{\alpha}^{Nmol}\sum_{i_\alpha}^{Np}\sum_{j_\alpha}^{Np} V^R(r_{i\alpha j\alpha}) - \sum_{\alpha}^{Nmol}\sum_{i\alpha}^{Np}\sqrt{\sum_{j_\alpha}^{Np} V^A(r_{i\alpha j\alpha})} \tag{A.11}$$

$$\frac{dV_{sc}}{d\mathbf{r}_s} = -\frac{1}{2}\sum_{\alpha}^{Nmol}\sum_{i_\alpha}^{Np}\sum_{j_\alpha}^{Np} F^R(r_{i_\alpha j_\alpha}) + \frac{1}{2}\sum_{\alpha}^{Nmol}\sum_{i_\alpha}^{Np}\left[\frac{1}{\sqrt{\sum_{j_\alpha}^{Np} V^A(r_{i_\alpha j_\alpha})}}\left(\frac{d\sum_{j_\alpha}^{Np} V^A(r_{i_\alpha j_\alpha})}{d\mathbf{r}_s}\right)\right] \tag{A.12}$$

note that

$$\frac{d\mathbf{r}_{ij}}{d\mathbf{r}_s} = \hat{r}_{ij}\delta_{is} - \hat{r}_{ij}\delta_{js} \tag{A.13}$$

$$\frac{dV_{sc}}{d\mathbf{r}_s} = -\frac{1}{2}\sum_{\alpha}^{Nmol}\sum_{i_\alpha}^{Np}\sum_{j_\alpha}^{Np} F^R(r_{i_\alpha j_\alpha}) - \frac{1}{2}\sum_{\alpha}^{Nmol}\sum_{i_\alpha}^{Np}\sum_{j_\alpha}^{Np}\left[\frac{1}{\sqrt{\sum_{j_\alpha}^{Np} V^A(r_{i_\alpha j_\alpha})}}\left(V^{A'}(r_{i_\alpha j_\alpha})\frac{\mathbf{r}_{i_\alpha j_\alpha}}{r_{i_\alpha j_\alpha}}\delta_{i_\alpha s} - V^{A'}(r_{i_\alpha j_\alpha})\frac{\mathbf{r}_{i_\alpha j_\alpha}}{r_{i_\alpha j_\alpha}}\delta_{j_\alpha s}\right)\right] \tag{A.14}$$

$$\frac{dV_{sc}}{d\mathbf{r}_s} = -\frac{1}{2}\sum_{\alpha}^{Nmol}\sum_{i_\alpha}^{Np}\sum_{j_\alpha}^{Np} F^R(r_{i_\alpha j_\alpha}) - \frac{1}{2}\sum_{\alpha}^{Nmol}\sum_{i_\alpha}^{Np}\sum_{j_\alpha}^{Np}\frac{1}{\sqrt{\sum_{j_\alpha}^{Np} V^A(r_{i_\alpha j_\alpha})}}V^{A'}(r_{i_\alpha j_\alpha})\hat{r}_{i_\alpha j_\alpha} + \frac{1}{\sqrt{\sum_{i_\alpha}^{Np} V^A(r_{i_\alpha j_\alpha})}}V^{A'}(r_{i_\alpha j_\alpha})\hat{r}_{j_\alpha i_\alpha} \tag{A.15}$$

$$\frac{dV_{sc}}{d\mathbf{r}_s} = -\frac{1}{2}\sum_{\alpha}^{Nmol}\sum_{i_\alpha}^{Np}\sum_{j_\alpha}^{Np} F^R(r_{i_\alpha j_\alpha}) - \frac{1}{2}\sum_{\alpha}^{Nmol}\sum_{i_\alpha}^{Np}\sum_{j_\alpha}^{Np}\left(\frac{1}{\sqrt{\sum_{j_\alpha}^{Np} V^A}} + \frac{1}{\sqrt{\sum_{i_\alpha}^{Np} V^A}}\right)V^{A'}\hat{r}_{i_\alpha j_\alpha} \tag{A.16}$$

$$\frac{dV_{sc}}{dt} = -\frac{1}{2}\sum_{\alpha}^{Nmol}\sum_{i_\alpha}^{Np}\sum_{j_\alpha}^{Np} F^R(r_{i_\alpha j_\alpha}).\left(\mathbf{v}_{i_\alpha} - \mathbf{v}_{j_\alpha}\right) + \frac{1}{2}\sum_{\alpha}^{Nmol}\sum_{i_\alpha}^{Np}\sum_{j_\alpha}^{Np} F^A(r_{i_\alpha j_\alpha}).\left(\mathbf{v}_{i_\alpha} - \mathbf{v}_{j_\alpha}\right) = -\frac{1}{2}\sum_{\alpha}^{Nmol}\sum_{i_\alpha}^{Np}\sum_{j_\alpha}^{Np} F_{sc}.(\mathbf{v}_{i_\alpha} - \mathbf{v}_{j_\alpha}) \tag{A.17}$$

$$\frac{dE_{sc}}{dt} = \sum_{\alpha}^{Nmol}\sum_{i_\alpha}^{Np}\sum_{j_\alpha}^{Np} F_{sc}.\mathbf{v}_{i_\alpha} + \frac{dV_{sc}}{dt}$$
$$= \sum_{\alpha}^{Nmol}\sum_{i_\alpha}^{Np}\sum_{j_\alpha}^{Np} F_{sc}.\mathbf{v}_{i_\alpha} - \frac{1}{2}\sum_{\alpha}^{Nmol}\sum_{i_\alpha}^{Np}\sum_{j_\alpha}^{Np} F_{sc}.(\mathbf{v}_{i_\alpha} - \mathbf{v}_{j_\alpha}) = \frac{1}{2}\sum_{\alpha}^{Nmol}\sum_{i_\alpha}^{Np}\sum_{j_\alpha}^{Np} F_{sc}.(\mathbf{v}_{i_\alpha} + \mathbf{v}_{j_\alpha}) \quad \text{(A.18)}$$

$$\frac{d\mathbf{G}_{sc}}{dt} = \frac{1}{2}\sum_{\alpha}^{Nmol}\sum_{i_\alpha}^{Np}\sum_{j_\alpha}^{Np} \mathbf{r}_{i_\alpha}[F_{sc}.(\mathbf{v}_{i_\alpha} + \mathbf{v}_{j_\alpha})]$$
$$= \frac{1}{4}\sum_{\alpha}^{Nmol}\sum_{i_\alpha}^{Np}\sum_{j_\alpha}^{Np} \mathbf{r}_{i_\alpha}[F_{sc}.(\mathbf{v}_{i_\alpha} + \mathbf{v}_{j_\alpha})] + \frac{1}{4}\sum_{\alpha}^{Nmol}\sum_{i_\alpha}^{Np}\sum_{j_\alpha}^{Np} \mathbf{r}_{j_\alpha}[F_{sc}.(\mathbf{v}_{j_\alpha} + \mathbf{v}_{i_\alpha})] \quad \text{(A.19)}$$

$$\mathbf{j}_{sc} = \frac{1}{2}\sum_{\alpha}^{Nmol}\sum_{i_\alpha<j_\alpha}^{Np} \mathbf{r}_{i_\alpha j_\alpha}[\mathbf{F}_{sc}(r_{i_\alpha j_\alpha}).(\mathbf{v}_{i_\alpha} + \mathbf{v}_{j_\alpha})] \quad \text{(A.20)}$$

CURRICULUM VITAE

Ceren Ece YÜCE:

EDUCATION:

- **B.Sc.:** 2020, İstanbul Technical University, Faculty of Science and Letters, Department of Physics Engineering

PROFESSIONAL EXPERIENCE AND REWARDS:

- 2017 TUBİTAK MAM
- 2018 TUBİTAK UME
- 2020 Research Assistant at İstanbul Technical University

PUBLICATIONS, PRESENTATIONS AND PATENTS ON THE THESIS:

- **Yüce C. E.**, Servantie C. (2022). Computation of thermal conductivity in nanofluids. *THE INTERNATIONAL GRADUATE RESEARCH SYMPOSIUM(IGRS'22)*, June 1-3, 2022 İstanbul, Turkey. (Presentation Instance)